Absolute Configuration of Bilirubin Conformational Enantiomers

Stefan E. Boiadjiev,[1a] Richard V. Person,[1a] Gisbert Puzicha,[1a] Carolyn Knobler,[1b] Emily Maverick,[1b] Kenneth N. Trueblood,[1b] and David A. Lightner*,[1a]

Contribution from the Department of Chemistry, University of Nevada, Reno, Nevada 89557-0020, and Department of Chemistry and Biochemistry, University of California, Los Angeles, California 90024. *Received March 26, 1992*

Abstract: Bilirubin, the yellow pigment of jaundice, is a bichromophoric tetrapyrrole formed in mammals by heme catabolism. It readily adopts either of two enantiomeric folded conformations which are shaped like ridge tiles and are stabilized by a network of intramolecular hydrogen bonds. Interconversion of the conformational enantiomers is rapid at room temperature and may be displaced toward either enantiomer by complexation with chiral agents. Intramolecular steric effects may also affect enantioselection. Thus, introduction of a methyl group at each of the β- and β'-carbons of the propionic acid chains on the symmetric bilirubin analog, mesobilirubin XIIIα, can shift the conformational equilibrium toward either the *M*- or the *P*-chirality intramolecularly hydrogen-bonded conformer, depending only on the *R* or *S* stereochemistry at β and β'. With the appropriate *R* or *S* configurations, intense bisignate circular dichroism (CD) may be detected for the ~430-nm transition(s) that is characteristic of exciton coupling between the component dipyrrinone chromophores. The absolute configuration of the β,β'-dimethylmesobilirubin XIIIα exhibiting a negative chirality CD exciton couplet ($\Delta\epsilon_{434}^{max}$ -337, $\Delta\epsilon_{390}^{max}$ +186 in $CHCl_3$) is firmly established as $\beta S,\beta' S$ by X-ray crystallography of the brucine salt of a monopyrrole synthetic precursor, (+)-(*S*)-3-[2,4-dimethyl-5-(ethoxycarbonyl)-1*H*-pyrrol-3-yl]butanoic acid (**5**). Molecular dynamics calculations on the $\beta S,\beta' S$ enantiomer confirm a strong preference (~20 kcal/mol stabilization) for intramolecularly hydrogen-bonded conformational enantiomers in which the *M*-chirality is favored over the *P*-chirality (by ~4 kcal/mol). For the first time, the absolute configuration of a bilirubin ridge-tile conformational enantiomer has been unequivocally established.

Introduction

Bilirubin (Figure 1), the cytotoxic yellow-orange tetrapyrrole pigment of jaundice[2,3] consists of two dipyrrinone units conjoined by a $-CH_2-$ group at C-10. As in structurally simpler molecular propellers, such as diphenylmethane,[4] rotation of the dipyrrinones about the bonds to the central $-CH_2-$ generates a large array of conformations, one of which is unique in being near or at the global energy minimum[5,6] and, particularly, in positioning the propionic acid -COOH group of one dipyrrinone unit in an ideal location for intramolecular hydrogen bonding with the pyrrole and lactam N—H and C=O residues of the other dipyrrinone. Stabilization of this conformation by a complementary network of intramolecular hydrogen bonds was first detected in the solid (by X-ray crystallography),[7] where bilirubin is folded into either of two ridge-tile-shaped enantiomers (Figure 1). Intramolecular hydrogen bonding has also been detected in solution by NMR,[8,9] where the bilirubin conformers are thought to persist as a pair of interconverting conformational enantiomers[2,10] in solvents that do not strongly perturb the matrix of intramolecular hydrogen bonds. Although the situation is less clear for solvents or other agents that may disrupt the folded pigment's hydrogen-bonding matrix, in the strong hydrogen bond acceptor $(CD_3)_2SO$, ^{13}C-NMR analysis of segmental motion in the propionic acid chains indicates that the -COOH residues are tethered to the dipyrrinones via bound solvent molecules.[11] Although it is probably folded,[12] the precise conformation of the pigment in $(CH_3)_2SO$ is uncertain.[13]

Molecular dynamics calculations on bilirubin confirm the importance of intramolecular hydrogen bonding. The conformational energy map (Figure 2) for rotations of the dipyrrinones about C-10 reveals a collection of isoenergetic global minima, which correspond to either identical or mirror image structures represented by the *M*- and *P*-chirality conformers of Figure 1. Interestingly, aside from differences due to enantiomerism, the global energy minimum conformation of bilirubin is essentially the same, whether hydrogen bonding is present or absent. Thus, with full hydrogen bonding, the global energy minimum for the *P*-chirality conformer lies at $\phi_1 = \phi_2 = 64°$; in the absence of hydrogen bonding, it lies at $\phi_1 = \phi_2 \simeq 70°$. However, the stabilization due to intramolecular hydrogen bonding is potentially considerable, which we estimate to be ~20 kcal/mol. This suggests that other conformers are essentially absent and that studies of bilirubin conformation should, as a starting point, focus on intramolecularly hydrogen-bonded structures.

The "internal" stereochemistry and nonbonded steric interactions in the intramolecularly bonded conformers are quite revealing. Close inspection of the steric environment of each of the diastereotopic hydrogens in the $-CH_2-CH_2-$ fragment of the intramolecularly hydrogen-bonded propionic acid groups suggests a way to displace the $M \rightleftarrows P$ equilibrium of Figure 1. Thus, when folded into the *M*-chirality ridge-tile enantiomer, the *pro-R* β-hydrogen (but not the *pro-S*) is brought into close nonbonded contact with the central $-CH_2-$ group at C-10, as illustrated in Figure 3 for the symmetric bilirubin analog, mesobilirubin XIIIα.

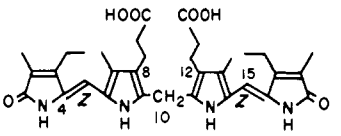

Mesobilirubin-XIIIα

On the other hand, in the *P*-chirality enantiomer, it is the *pro-S* β-hydrogen that is buttressed against the C-10 $-CH_2-$ group. Consequently, when mesobilirubin or bilirubin adopts either of the thermodynamically preferred intramolecularly hydrogen-

(1) (a) University of Nevada. (b) University of California.
(2) Lightner, D. A.; McDonagh, A. F. *Acc. Chem. Res.* **1984**, *17*, 417-424.
(3) For leading references, see: Gollan, J. L. (Guest Ed.). *Seminars in Liver Disease* **1988**, *8*, 103-199, 272-283.
(4) Barnes, J. C.; Paton, J. D.; Damewood, J. R., Jr.; Mislow, K. *J. Org. Chem.* **1981**, *46*, 4975-4979.
(5) For leading references, see: Falk, H. *The Chemistry of Linear Oligopyrroles and Bile Pigments*; Springer-Verlag: Wien, New York, 1989.
(6) Lightner, D.; Person, R.; Peterson, B.; Puzicha, G.; Pu, Y.-M.; Bojadziev, S. In *Biomolecular Spectroscopy II*; Birge, R., Nafie, L., Eds.; Proc. SPIE-The International Society for Optical Engineering, Bellingham, WA, 1432; 1991; pp 2-3.
(7) (a) Bonnett, R.; Davies, J. E.; Hursthouse, M. B.; Sheldrick, G. M. *Proc. R. Soc. London, B* **1978**, *202*, 249-268. (b) LeBas, G.; Allegret, A.; Mauguen, Y.; DeRango, C.; Bailly, M. *Acta Crystallogr., Sect. B* **1980**, *B36*, 3007-3011.
(8) Trull, F. R.; Ma, J.-S.; Landen, G. L.; Lightner, D. A. *Isr. J. Chem.* **1983**, *23*, 211-218.
(9) Kaplan, D.; Navon, G. *Isr. J. Chem.* **1983**, *23*, 177-186.
(10) (a) Manitto, P.; Monti, D. *J. Chem. Soc., Chem. Commun.* **1976**, 122-123. (b) Navon, G.; Frank, S.; Kaplan, D. *J. Chem. Soc., Perkin Trans 2* **1984**, 1145-1149.
(11) Kaplan, D.; Navon, G. *Biochem. J.* **1982**, *201*, 605-613.
(12) Gawroński, J. K.; Połonski, T.; Lightner, D. A. *Tetrahedron* **1990**, *24*, 8053-8066.
(13) Hsieh, Y.-Z.; Morris, M. D. *J. Am. Chem. Soc.* **1988**, *110*, 62-67.

0002-7863/92/1514-10123$03.00/0

bonded ridge-tile conformations, one conformational enantiomer can be destabilized relative to the other through allosteric action by judicious replacement of hydrogens on the propionic acid chain by methyl groups. For example, insertion of a methyl group at the *pro-S* site on the β-carbon of the propionic acid would be expected to destabilize the *P*-chirality intramolecularly hydrogen-bonded conformational enantiomer by introducing a severe nonbonded $CH_3|CH_2$ steric interaction with the C-10 $-CH_2-$ group (Figure 4). This would shift the conformational equilibrium toward *M*. In contrast, introduction of a methyl group at the *pro-R* site would destabilize the *M*-chirality enantiomer and shift the equilibrium toward *P*. Introduction of such methyl groups might thus be expected to force the resolution of bilirubin through intramolecular steric interaction, assuming that intramolecular hydrogen bonding remains a potent conformation-stabilizing force. In order to examine this principle, we targeted the synthesis of a bilirubin analog, β,β′-dimethylmesobilirubin XIIIα (**1**), where we could achieve an optical resolution and determine the absolute configuration at an early step.

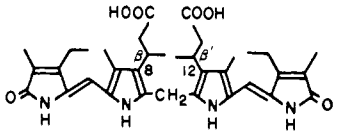

β,β′-Dimethylmesobilirubin-XIIIα

In the following, we report on the total synthesis and circular dichroism of the bilirubin analog (−)-(β*S*,β′*S*)-dimethylmesobilirubin XIIIα (**1a**) and on the X-ray crystallographic determination of the absolute configuration of its precursor (+)-(*S*)-3-[2,4-dimethyl-5-(ethoxycarbonyl)-1*H*-pyrrol-3-yl]butanoic acid (**5a**), as the brucine salt. These results are important because (i) they present an unequivocal experimental determination of the absolute configuration as *M*-helicity for the negatively rotating bilirubin conformational enantiomer, (ii) they confirm the presence and significance of intramolecular hydrogen bonding in stabilizing conformation, and (iii) they provide useful molecular models for assessing the structure of bilirubin in biological tissues and fluids.

Results and Discussion

Synthesis. A stereospecific total synthesis of the *S*,*S* and *R*,*R* enantiomers of β,β′-dimethylmesobilirubin XIIIα was devised in which enantiomeric resolution was achieved at the monopyrrole stage. The stereogenic centers (β,β′) found in the target pigment **1** are carried along by monopyrrole precursor **6** (Scheme I) and originate early in the synthesis, having been introduced by a Michael reaction of pentane-2,4-dione with methyl crotonate. When racemic (*R*,*S*)-**6** is converted ultimately into **1**, two diastereomers are obtained: the meso diastereomer (**1c**), which has the *R*,*S* configuration at the β,β′-centers, and the racemic diastereomer (**1a** + **1b**), which consists of the *R*,*R* and *S*,*S* enantiomers. Diastereomer **1c** amounts to 50% of the mixture and can be separated from (**1a** + **1b**) by chromatography.

The target optically active compounds (β*S*,β′*S*)- and (β*R*,-β′*R*)-dimethylmesobilirubin XIIIα (**1a** and **1b**) were prepared from optically active precursors **5a** and **5b**, respectively (Scheme I), which were resolved to 100% and 80% enantiomeric excess (ee), respectively, by fractional crystallization of the brucine salts. Thus, **5a** could be saponified to diacid **4a**, which, upon heating with (bromomethylene)oxopyrrole **7**[14] in refluxing CH_3OH, gave dipyrrinone **3a** ($[\alpha]^{20}_D$ +61.8° (*c* 0.8, $CHCl_3$)). Chloranil-promoted oxidative coupling[15] of **3a** afforded the mesobiliverdin dimethyl ester **2a** ($[\alpha]^{20}_{436}$ −2720° (*c* 0.0037, $CHCl_3$)). After saponification of **2a**, $NaBH_4$ reduction yielded **1a** ($[\alpha]^{20}_D$ −4730° (*c* 0.0086, $CHCl_3$)). Synthesis of racemic **6** was accomplished by Fischer–Knorr type condensation[14] of nitrosated ethyl acetoacetate and methyl 4-acetyl-3-methyl-5-oxohexanoate in 20% yield. The atypically low yield was caused, presumably, by the introduction of steric ortho type hindrance between the propionic acid β-methyl group and the pyrrole ring methyls at C-2 and C-4. A better alternative involved condensation of nitrosated diethyl malonate in place of nitrosated ethyl acetoacetate, and this reaction gave **6** in 60% yield. Diester **6** was selectively saponified to give racemic monoacid **5**, which was resolved as the 1:1 salt with brucine·$4H_2O$ by fractional crystallization from acetone until the acid (**5a**) maintained a constant rotation, $[\alpha]^{20}_D$ +30.5° (*c* 0.8, ethanol). The absolute configuration of the highly resolved acid was determined by X-ray crystallography (below) of its 1:1 salt with brucine. Highly resolved enantiomeric acid **5b**, $[\alpha]^{20}_D$ −24.4° (*c* 1.3, ethanol), was obtained from the mother liquors by repeated fractional crystallization, and it was converted to (β*R*,β′*R*)-dimethylmesobilirubin XIIIα (**1b**), $[\alpha]^{20}_D$ = +4880° (*c* 0.0075, $CHCl_3$), as outlined in Scheme I.

The synthesis of **1b** illustrates an interesting principle, which results in *resolution by synthesis*. When **5b** of 80% ee is carried through the synthetic scheme, the coupling step that converts dipyrrole **3** to tetrapyrrole **2** presents an opportunity for increasing the ee of the desired product (**1b**). Assuming equal rates of coupled oxidation, **3b** with 80% ee should give **2** containing the statistical mixture of isomers: 81% **2b**, 1% **2a**, and 18% **2c**. In fact, this is essentially what we find, and since the meso diastereomer **1c** derived from **2c** can be removed easily at the final product stage (**1**), the desired product (**1b**) can be obtained very simply in >97% ee starting with **5b** of only 80% ee.

Molecular Geometry and Absolute Configuration from X-ray Crystallography. In the 1:1 salt of **5a** with brucine, a water molecule links the cation and the anion via the brucine amide O and a pyrrole acid O (Figure 5), with nearly linear H-bonds. The other acid O is H-bonded to the $-NH^+$ of a second brucine cation,

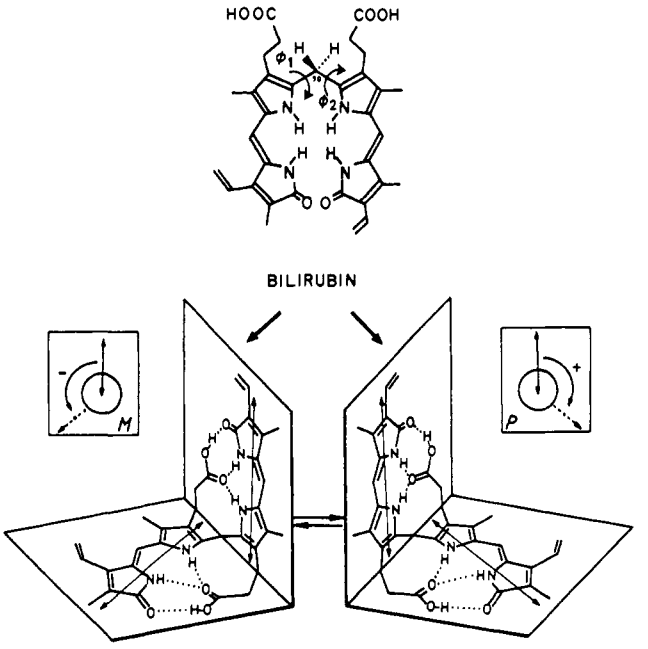

Figure 1. (Upper) Porphyrin-like representation of (4*Z*,15*Z*)-bilirubin IXα, whose two dipyrrinone chromophores are connected by a $-CH_2-$ group. Rotation of the two dipyrrinones, like propeller blades, about the central $-CH_2-$ (rotation angles ϕ_1 and ϕ_2) converts this nearly planar shape ($\phi_1 = \phi_2 = 0°$) into a folded shape in which the propionic acid groups are brought into sufficiently close nonbonded proximity ($\phi_1 = \phi_2 \simeq 60°$ for *P*, and $\phi_1 = \phi_2 \simeq -60°$ for *M*) to facilitate intramolecular hydrogen bonding to the opposing dipyrrinone lactam and pyrrole groups. (Lower) Three-dimensional representations for two enantiomeric intramolecularly hydrogen-bonded conformations, which are shaped like ridge tiles. These conformers interconvert by breaking a set of hydrogen bonds and then rotating one dipyrrinone about C-10 followed by re-forming the hydrogen bonds. (Inset) The chirality or helicity of the two enantiomers is shown as *M* or *P*, according to the relative helical orientation of the long wavelength (~430 nm) transition induced electric dipole moments that are oriented along the long axis of each of the two dipyrrinone chromophores of each molecule.

(14) Shrout, D. P.; Lightner, D. A. *Synthesis* **1990**, 1062–1065.
(15) Shrout, D. P.; Puzicha, G.; Lightner, D. A. *Synthesis* **1992**, 328–332.
(16) Trull, F. R.; Franklin, R. W.; Lightner, D. A. *J. Heterocycl. Chem.* **1987**, *24*, 1573–1579.

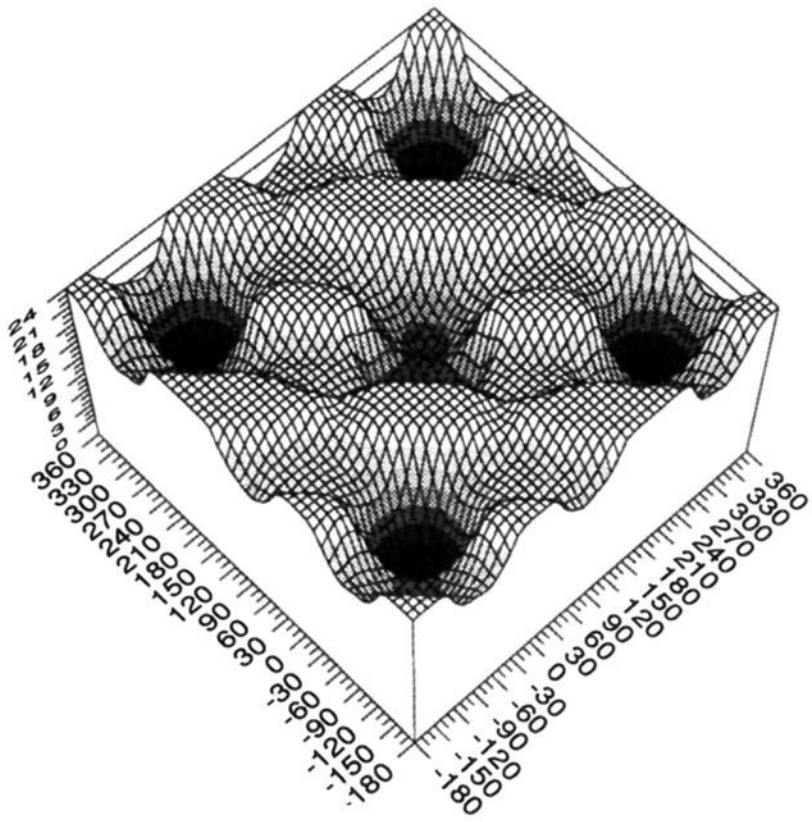

Figure 2. (Upper) Potential energy surface and (lower) contour maps for bilirubin IXα conformations generated by rotating the two dipyrrinone groups independently about the C-9–C-10 and C-10–C-11 bonds (ϕ_1 and ϕ_2, respectively). The energy scale (bottom) is in kcal/mol, and global minima (set to 0 kcal/mol) are found near $(\phi_1,\phi_2) \simeq (60°,60°)$ (*P*-chirality) and $(\phi_1,\phi_2) \simeq (-60°,-60°)$, $(-60°,300°)$, $(300°,-60°)$, $(300°,300°)$ (*M*-chirality). Data are from molecular dynamics simulations using SYBYL (Tripos Associates) on an Evans & Sutherland ESV-10 workstation.

as well as the –NH of another anion. The structure contains one molecule of water, and also one molecule of acetone, for each 1:1 salt; the acetone molecule is not, however, involved in any hydrogen bonding. The geometry of the brucinium ion is not significantly different from that reported for the neutral molecule,[17] the only appreciable discrepancies in distances (up to 0.03 Å) occurring in the vicinity of the tertiary N atom, which is protonated in the present structure. The five atoms of the pyrrole ring of **5a** are coplanar (maximum deviation 0.003 Å); the four C atoms attached

(17) Glover, S. S. B.; Gould, R. O.; Walkinshaw, M. D. *Acta Crystallogr.* **1985**, *C41*, 990–994.

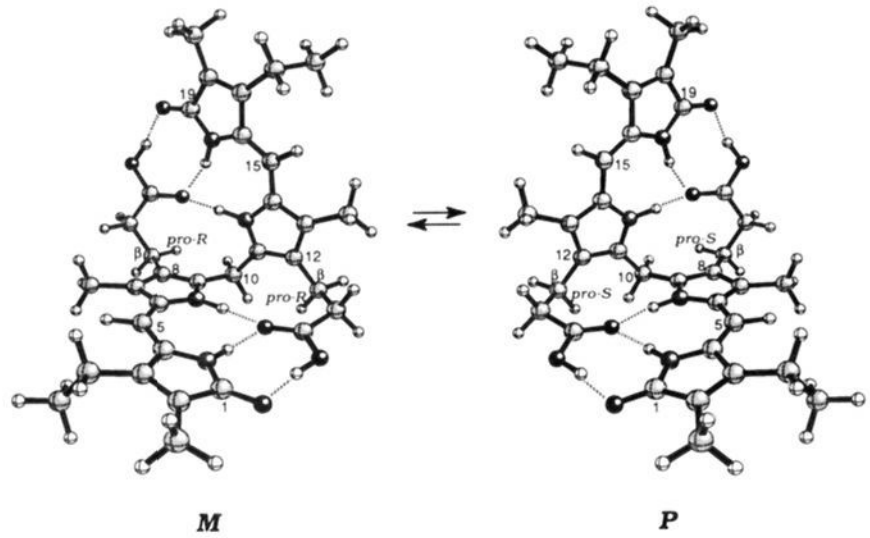

Figure 3. Ball and stick conformational representations for the ridge-tile shape *M*- and *P*-chirality intramolecularly hydrogen-bonded, interconverting enantiomers of mesobilirubin XIIIα. In the propionic acid side chains attached to pyrrole ring carbons C-8 and C-12, the hydrogens on the β and β' $-CH_2-$ groups are either *pro-R* or *pro-S* (only one hydrogen of the set is designated). When the *M*-chirality conformer inverts into the *P*-chirality, steric crowding of the *pro-R* hydrogens is relieved and replaced by similar crowding of the *pro-S* hydrogens.

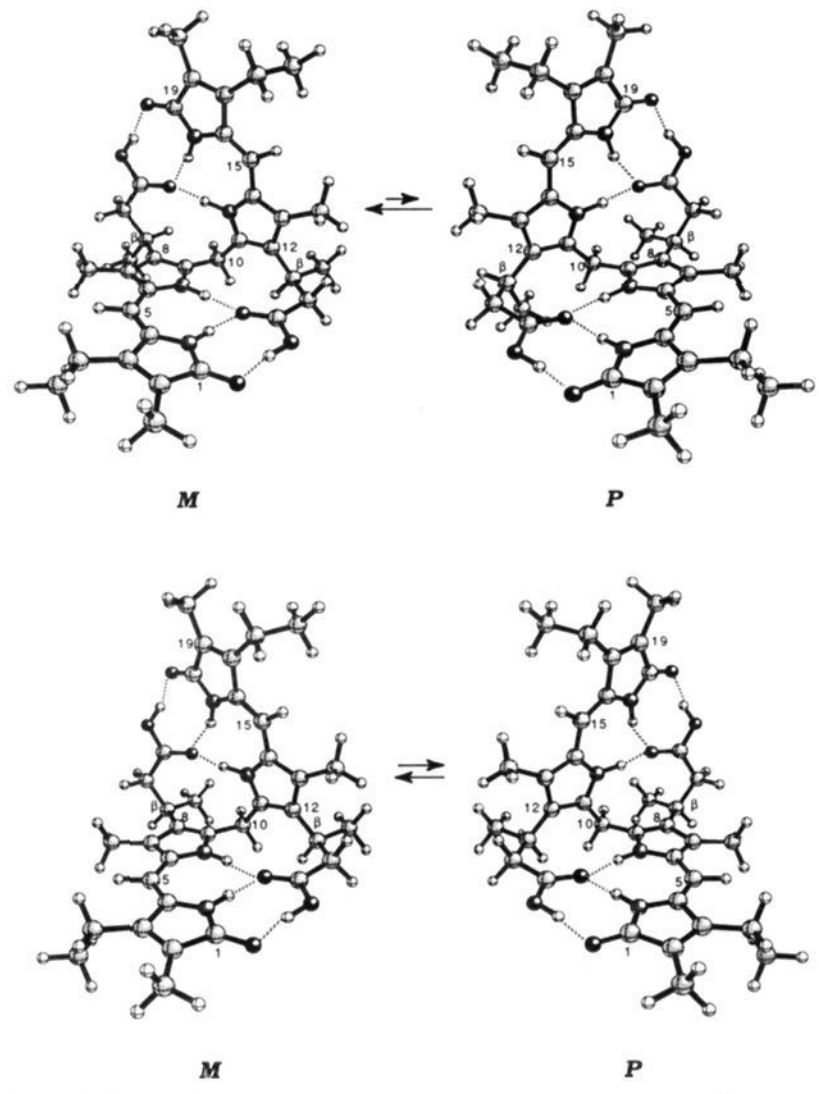

Figure 4. Ball and stick representations for the most stable conformations of (upper) ($\beta S,\beta' S$)-dimethylmesobilirubin XIIIα (**1a**) and (lower) ($\beta S,\beta' R$)-dimethylmesobilirubin XIIIα (**1c**) in their ridge-tile shape, *M*- and *P*-chirality intramolecularly hydrogen-bonded diastereomers. In the *M*-chirality diastereomer of **1a** (upper left), the ($\beta S,\beta' S$)-methyl groups lie away from the C-10 $-CH_2-$ group, but in the less stable (4.3 kcal higher energy) *P*-chirality diastereomer (upper right), the methyls are buttressed against the C-10 $-CH_2-$. In contrast, the *M*- and *P*-chirality conformations of the meso diastereomer (**1c**) (lower) are identical, with each having one β-methyl at an unhindered site and the other at a sterically hindered site. These conformations lie ~2.2 kcal/mol higher in energy than *M*-**1a** but ~2.1 kcal/mol lower than *P*-**1a**.

to this ring are bent away from the best plane in the same direction, by 0.04–0.14 Å. The molecular geometry of **5a** seems unexceptionable.

The absolute configuration of **5a** is determined as *S*, from the known configuration of the naturally occurring (–)-brucine[17] used to form the 1:1 salt. Since **5a** is converted to dipyrrinone **3a**,

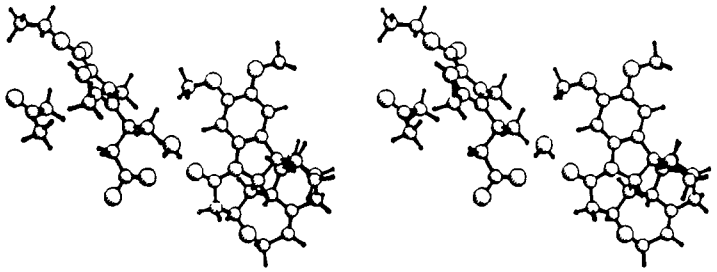

Figure 5. Stereoview of the mutual arrangement of the components of the crystal. The brucinium cation is on the right, and the anion of **5a** on the left. The water molecule that forms the hydrogen-bonding link between these ions is clearly evident. The acetone molecule is at the far left. The ratios of the radii used for O, N, and C atoms in this PLUTO[27] drawing are respectively 9:8:7.

Scheme I

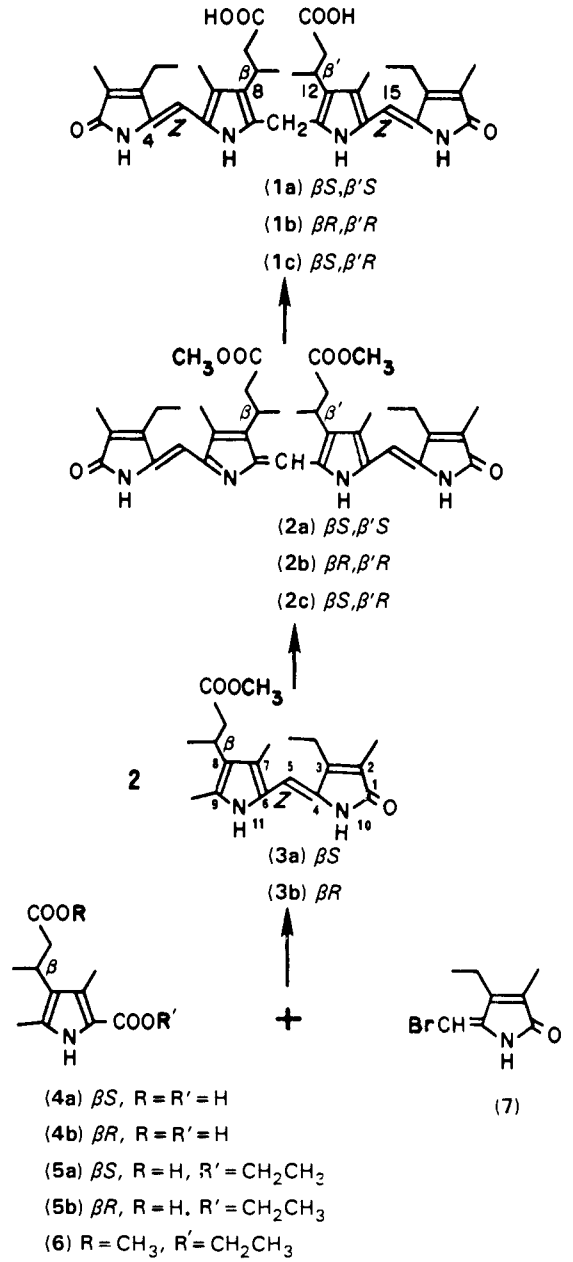

mesobiliverdin **2a**, and mesobilirubin **1a** without inversion of configuration, it follows that they, too, must be assigned the *S* stereochemistry at their stereogenic center(s). We accordingly, assign the *R,R* absolute stereochemistry to enantiomer **1b**.

Properties. The chromatographic properties of **1a** or **1b** on TLC and on HPLC (R_f 0.62, retention time 32.0 min) were very similar

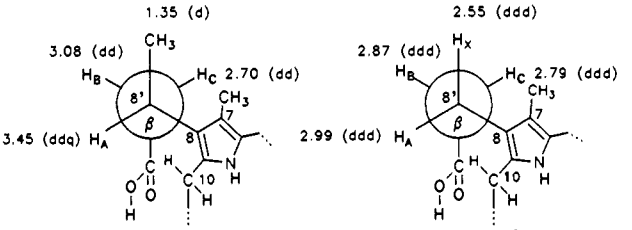

Figure 6. Newman projections for the propionic acid residues in (βS,-$\beta' S$)-dimethylmesobilirubin XIIIα (**1a**) (left) and in mesobilirubin XIIIα (right). The chemical shifts and splittings are assigned to the relevant protons on the basis of earlier assignments for bilirubin.[10b]

to those previously observed for mesobilirubin XIIIα (R_f 0.55, retention time 8.7 min) and bilirubin (R_f 0.68, retention time 8.9 min), consistent with the picture (Figure 1) where the polarity is reduced through intramolecular hydrogen bonding. The meso diastereomer **1c** was more polar (R_f 0.38, retention time 16.6 min) and could be separated from the racemic diastereomer (**1a** + **1b**) by chromatography or extraction into bicarbonate. The greater polarity of the meso diastereomer is explained as follows. When the configurations at the propionic acid β- and β'-carbons are not the same as is the case in the *R,S* diastereomer, equivalent nonbonded destabilizing steric interactions between these CH_3 groups and the C-10 $-CH_2-$ group are introduced into both the *M* and *P* conformational diastereomers. That is, although a (βR)-CH_3 group on one propionic acid chain would fit comfortably in the *P*-chirality intramolecularly hydrogen-bonded conformer, the ($\beta' S$)-CH_3 on the other propionic acid chain would not. Similarly, although the (βS)-CH_3 group would fit comfortably in the *M*-chirality conformer, the ($\beta' R$)-CH_3 would not. This steric destabilization yields conformations in which at least one propionic acid group is not as strongly involved as the other in intramolecular hydrogen bonding, hence the increased polarity, different solubility, and chromatographic properties of the meso diastereomer. These differences, which suggest different conformations in solution, are also manifested in the pigment's NMR spectra, as explained below.

Conformation and Hydrogen Bonding. Intramolecular hydrogen bonding is thought to be the most important factor in stabilizing the folded, ridge-tile conformation of bilirubin in the crystal[5,7] and in solution in nonpolar solvents.[5,8-11] It is thought to be important even in polar and hydroxylic solvents,[5,11] and it is of major importance to the success of the allosteric model presented in this work. The potential for intramolecular hydrogen bonding in mesobilirubin **1a** or **1b** differs little from that of bilirubin or mesobilirubin XIIIα, and as with these pigments, the conformations of the β,β'-dimethylmesobilirubins can be deduced from NMR experiments in $CDCl_3$.[10] The ^{1}H-NMR data (Table I) for (**1a** + **1b**) may be compared with those of the parent, mesobilirubin XIIIα, which has no β,β'-methyl groups. Predictably, the proton chemical shifts are very similar. Of special importance are the lactam and pyrrole N-*H* and carboxylic acid COO*H* chemical shifts in $CDCl_3$, a solvent in which intramolecular hydrogen bonding has previously been established for bilirubins. The strongly deshielded lactam N-*H* and COO*H* chemical shifts confirm the presence of hydrogen bonding, and the relatively more shielded pyrrole N-*H* chemical shifts are a strong indication of intramolecular hydrogen bonding,[8,9] as depicted in Figures 1 and 3, where one pyrrole N-*H* lies above the π-system of the other or where the pyrrole N-*H* is shielded by the carbonyl anisotropy.[18]

Further ^{1}H-NMR support for a stable, intramolecularly hydrogen-bonded ridge-tile conformation comes from analysis of vicinal H|H coupling in the propionic acid side chains. As expected for a conformation where the propionic acid residues are constrained to adopt fixed conformations, vicinal H|H coupling constants (**1a** + **1b** J_{AC} = 3 Hz, J_{AB} = 12 Hz; and mesobilirubin XIIIα J_{AC} = 3 Hz, J_{AB} = 13 Hz) in the propionic acid segments, $-CH_A(CH_3)-CH_BH_C-CO_2H$ and $-CH_AH_XCH_BH_CCO_2H$, respectively, are not the averaged values seen in flexible chains (cf.

(18) Karabatsos, G. J.; Sonnischen, G. C.; Hsi, N.; Fenoglio, D. J. *J. Am. Chem. Soc.* **1967**, *89*, 5067–5068.

Table I. Proton NMR Spectra (δ, ppm Downfield from $(CH_3)_4Si$) of Racemic (**1a** + **1b**) and Meso (**1c**) Diastereomers of β,β'-Dimethylmesobilirubin XIIIα in $CDCl_3$ and DMSO-d_6 at 22 °C

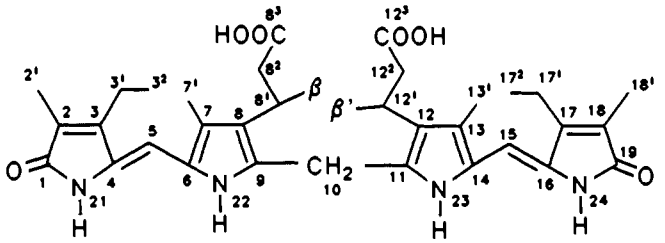

		(**1a** + **1b**)		(**1c**)		mesobilirubin XIIIα	
type	site	$CDCl_3$	DMSO-*d*	$CDCl_3$	DMSO-d_6	$CDCl_3$	DMSO-d_6
COOH	8^3,12^3	13.60 (s)	11.98 (brs)	13.73 (s) 13.3 (vbrs)	11.89 (brs)	13.31 (s)	11.87 (brs)
NH	21,24	10.68 (s)	9.85 (brs)	10.83 (s) 10.42 (s)	9.83 (brs)	10.52 (s)	9.74 (brs)
NH	22,23	9.04 (s)	10.10 (brs)	9.19 (s) 8.96 (s)	10.10 (brs)	9.15 (s)	10.28 (brs)
CH_3	β,β'	1.35 (d)[a]	0.98 (d)[f]	1.34 (d)[a] 1.70 (d)[a]	1.01 (d)[l]		
CH	8^1,12^1	3.45 (ddq)[b]	3.17 (dq)[g]	3.43 (m) 3.23 (m)	3.16 (dq)[m]	2.99 (ddd)[p] 2.56 (ddd)[q]	1.99 (t)[u]
CH_2	8^2,12^2	2.70 (dd)[c] 3.08 (dd)[d]	2.40 (dd)[h]	2.71 (dd)[j] 3.01 (dd)[i]	2.37 (dd)[n]	2.86 (ddd)[r] 2.79 (ddd)[s]	2.40 (t)[u]
CH_3	7^1,13^1	2.24 (s)	2.08 (s)	2.24 (s) 2.11 (s)	2.10 (s)	2.14 (s)	1.97 (s)
CH_2	3^1,17^1	2.48 (q)[e]	2.44 (q)[a]	2.48 (q)[e]	2.48 (m)	2.48 (q)[t]	2.49 (q)[t]
CH_3	3^2,17^2	1.11 (t)[e]	1.07 (t)[a]	1.11 (t)[e]	1.08 (t)[a]	1.12 (t)[t]	1.06 (t)[t]
CH_3	2^1,18^1	1.85 (s)	1.76 (s)	1.86 (s)	1.77 (s)	1.85 (s)	1.75 (s)
=CH	5,15	6.04 (s)	5.95 (s)	6.03 (s) 6.05 (s)	5.96 (s)	6.04 (s)	5.92 (s)
$-CH_2-$	10	4.06 (s)	3.98 (s)	4.40 (d)[k] 4.16 (d)[k]	3.87 (d)[o] 4.09 (d)[o]	4.06 (s)	3.93 (s)

[a] J = 7.4 Hz. [b] J = 3.0, 12.0, 7.4 Hz. [c] J = 3.0, 18.2 Hz and J = 18.2, 12.3 Hz. [d] J = 18.2, 12.3 Hz. [e] J = 7.6 Hz. [f] J = 7.0 Hz. [g] J = 8.1, 7.1 Hz. [h] J = 8.1, 8.1 Hz. [i] J = 4.1, 5.8 Hz. [j] J = 18.7, 3.4 Hz. [k] J = 15.8 Hz. [l] J = 6.7 Hz. [m] J = 7.7, 6.7 Hz. [n] J = 7.7, 7.7 Hz. [o] J = 16.7 Hz. [p] J = 13.4, 2.8, 14.9 Hz. [q] J = 14.9, 2.6, 4.7 Hz. [r] J = 13.4, 18.8, 2.6 Hz. [s] J = 2.8, 18.8, 4.7 Hz. [t] J = 7.2 Hz. [u] J = 7.8 Hz.

data in $(CD_3)_2SO$). They are consistent with a fixed and staggered segment geometry (Figure 6) with an H_A–C–C–H_C torsion angle of ~60° and an H_A–C–C–H_B torsion angle of ~180°, or close to the geometry seen in Dreiding models or in the global energy minimum conformation. And they indicate that the conformational enantiomerism depicted in Figures 1 and 3 is slow on the NMR time scale.[9,10]

The experimental evidence for intramolecular hydrogen bonding in **1a** is fully supported by molecular dynamics calculations, which show global energy minima (Figure 7) near ($\phi_1 = \phi_2 \simeq -60°$), ($\phi_1 \simeq -60°$, $\phi_2 \simeq 300°$), ($\phi_1 \simeq 300°$, $\phi_2 \simeq -60°$), and ($\phi_1 = \phi_2 \simeq 300°$), corresponding to the *M*-chirality conformer of Figure 4 (upper left). A local minimum corresponding to the *P*-chirality conformer of Figure 4 (upper right) is found near ($\phi_1 = \phi_2 \simeq 60°$) and lies some 4.3 kcal/mol higher in energy than that of the *M*-chirality due to nonbonded steric interactions between the β-methyls and the C-10 $-CH_2-$. Intramolecular hydrogen bonding remains an important factor despite the nonbonded steric interaction, but one conformational diastereomer (*M*) is clearly favored over the other (*P*). Secondary, higher energy local minima can be detected. One local minimum ($\phi_1 = \phi_2 \simeq 120°$) lies some 9.3 kcal/mol above the global minimum and located near the *P*-chirality minimum at ($\phi_1 = \phi_2 \simeq 60°$). Four isoenergetic local minima [($\phi_1 = \phi_2 \simeq -110°$), ($\phi_1 \simeq -110°$, $\phi_2 \simeq 250°$), ($\phi_1 = \phi_2 \simeq 250°$), and ($\phi_1 \simeq 250°$, $\phi_2 = -110°$)] lie some 11.2 kcal/mol higher in energy than the nearby *M*-chirality global minima. In these secondary local minima, residual hydrogen bonding is still maintained, as shown in Figure 8. However, in view of the predicted large energy difference between these secondary local minima and an *M*-chirality global minimum, they may be expected to contribute very little to the conformation of **1a**. Similarly, on the basis of energy considerations, the *P*-chirality conformer of **1a** probably contributes little to the overall conformation.

These conclusions reached above on the conformation of **1a** are supported additionally by ^{1}H-NMR NOE measurements. In the most stable *M*-chirality conformation (Figure 4, upper left) of **1a** (or *P*-chirality conformation of **1b**), the C-10 $-CH_2-$ lies close to the β,β'-hydrogens at C-8^1 and C-12^1 and distant from the β,β'-methyl groups at C-8^1 and C-12^1. One might therefore expect to see a strong NOE between the C-10 $-CH_2-$ hydrogens and the β,β'-hydrogens but no NOE, or at best a very weak NOE, for the β,β'-methyls. In fact, this is exactly what is observed: The signals at 3.45 ppm (hydrogens at C-8^1 and C-12^1, Table I) and those at 4.06 ppm (hydrogens at C-10) are related by a strong NOE, but the signals at 1.35 ppm (β-methyls at C-8^1 and C-12^1) and those at 2.24 ppm (pyrrole ring methyls, C-7^1 and C-13^1) show no NOE. In contrast, and as expected, strong NOEs can be found between the C-8^1, C-12^1 β,β'-methyls and the pyrrole ring C-7^1, C-13^1 methyls, but no NOEs can be found between the latter and the C-8^1, C-12^1 β,β'-hydrogens. These results are best accommodated by the intramolecularly hydrogen-bonded *M*-chirality conformation shown in Figure 4 for **1a**. Other strong NOEs found between lactam and pyrrole N*H*s, between the C-5, C-15 hydrogens and the C-3^1, C-17^1 $-CH_2-$, and between the C-5, C-15 hydrogens and the C-7^1, C-13^1 methyls confirm that the dipyrrinones of **1a** and **1b** adopt a syn-*Z* conformation, as indicated.

These data may be contrasted with those of the meso diastereomer **1c**, where only one propionic acid group can easily participate in the network intramolecular hydrogen bonds depicted in Figures 1 and 3. Tethering the remaining propionic acid to the opposing dipyrrinone through intramolecular hydrogen bonding compresses its β-methyl (located at C-8^1 or C-12^1) into the C-10 $-CH_2-$ (Figure 4, lower). Experimental evidence for intramolecular hydrogen bonding involving both propionic acid residues and both lactams comes from ^{1}H-NMR spectra of **1c** in $CDCl_3$ solvent (Table I). Two different deshielded CO_2H chemical shifts

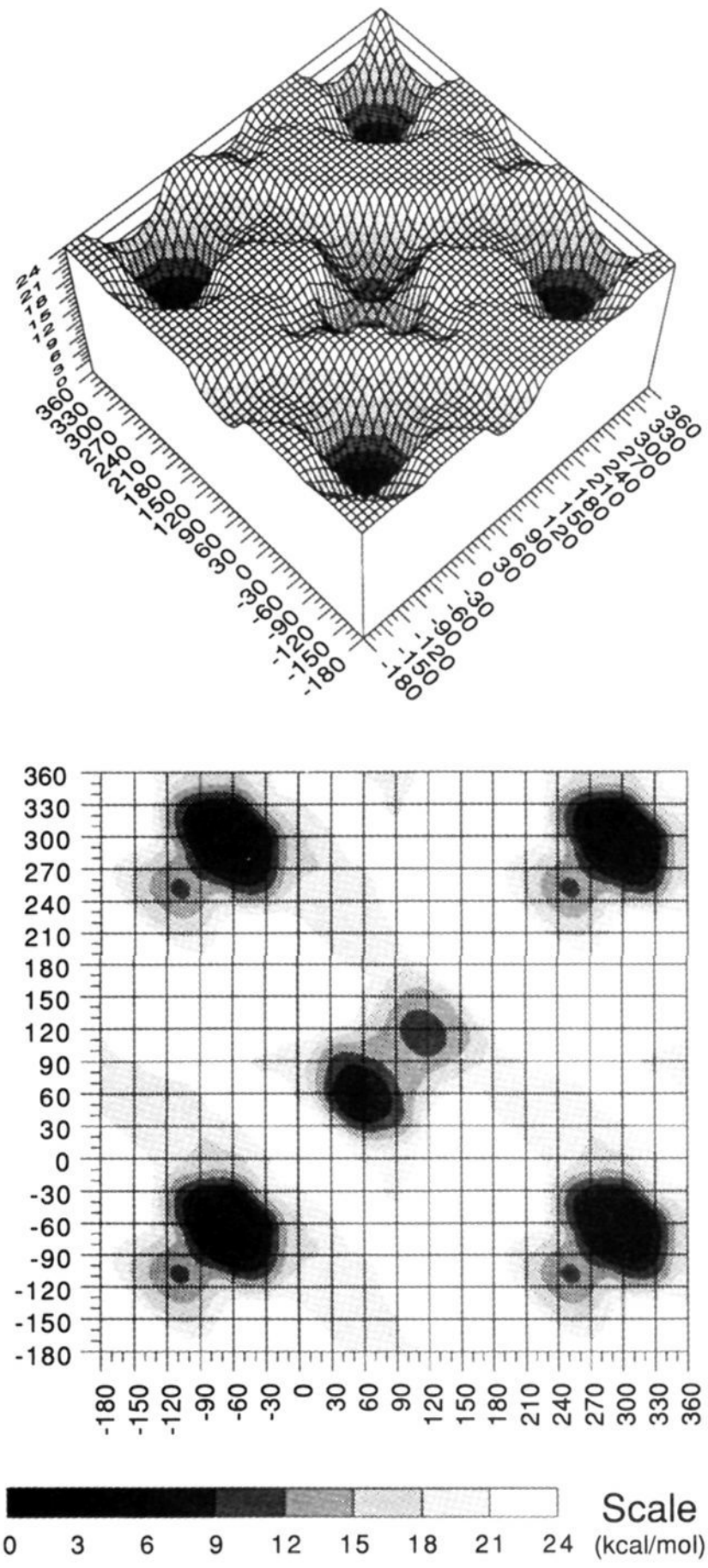

Figure 7. (Upper) Potential energy surface and (lower) contour maps for ($\beta S,\beta' S$)-dimethylmesobilirubin XIIIα (**1a**) conformations generated by rotating the two dipyrrinone groups independently about the C-9–C-10 and C-10–C-11 bonds (ϕ_1 and ϕ_2, respectively). The energy scale (bottom) is in kcal/mol, and global minima (set to 0 kcal/mol) are found near (ϕ_1,ϕ_2) = (−60°,−60°), (−60°,300°), (300°,−60°), and (300°,300°) (*M*-helicity). A local minimum is found near (ϕ_1,ϕ_2) = (60°,60°) (*P*-helicity) and lies ~4.3 kcal/mol above the global minima. The *P*-helicity minima are higher in energy than the *M*-helicity minimum because of the steric effects of the β-methyls interacting with the C-10 hydrogens. Data are from molecular dynamics simulations using SYBYL (Tripos Associates) on an Evans & Sutherland ESV-10 workstation.

are found at 13.73 and 13.3 ppm, with the former being near the 13.63 ppm value of **1a** and **1b** and the latter being broader than the more deshielded signal and presumably coming from the less tightly bound propionic acid group. The lactam N–*H* chemical shifts of **1c** (10.83 and 10.42 ppm) also flank those of (**1a** + **1b**) (10.68 ppm), with the more deshielded N–*H* probably coming from the more firmly hydrogen-bonded dipyrrinone. Also, as might be expected, the pyrrole N–*H* chemical shifts (9.19 and 8.96 ppm) of **1c** are close to those of **1a** + **1b** (9.04 ppm), and again, we attribute the more deshielded N–*H* to the dipyrrinone with the stronger hydrogen bonding. (For comparison, it may be noted that the N–*H* chemical shift of a model pyrrole, 2,4-dimethyl-3-ethylpyrrole, in $CDCl_3$ is ~7.2 ppm.[8]) The NMR data of **1c** are clearly consistent with the desymmetrized structure of **1c** in Figure 4. A symmetric (non-hydrogen-bonded) structure, such as the linear representation for **1c** (Scheme I), would not show the signal ^{1}H-NMR doublings seen in Table I and would not show the observed two distinct β-methyl signals. One methyl signal, presumably from the β-CH_3 of the more firmly hydrogen-bonded propionic acid residue, appears at 1.34 ppm, essentially the same as those in **1a** or **1b** (1.35 ppm) or in the precursor dipyrrinone (**3**), where the β-methyl resonance is at 1.29 ppm. In contrast, the other β-CH_3 of **1c** is more deshielded (1.70 ppm), apparently from steric compression into the C-10 –CH_2–. Reciprocally, the C-10 –CH_2– hydrogens in **1c** are also more deshielded than those of **1a** or **1b** and are no longer equivalent. The distinctions drawn from these resonances are consistent with the conformations shown in Figure 4 (lower) where one β-methyl lies very close to the C-10 –CH_2– and in especially close proximity to one of the –CH_2– hydrogens.

The conclusions reached above on the conformation of **1c** are supported by ^{1}H-NMR NOE studies in $CDCl_3$. NOEs are found between: (1) the C-8^1 or C-12^1 β H at 3.43 ppm and the C-10 hydrogen at 4.16 ppm; (2) the C-12^1 or C-8^1 β-H at 3.23 ppm and the $C_7{}^1$ or $C_{13}{}^1$ pyrrole ring CH_3 at 2.11 ppm; (3) the C-8^1 or C-12^1 β-CH_3 at 1.70 ppm and the C-10 hydrogen at 4.40 ppm; and (4) the C-12^1 or C-8^1 β-CH_3 at 1.34 ppm and the C-13^1 or C-7^1 pyrrole ring CH_3 at 2.24 ppm. They are also supported by molecular dynamics calculations. A conformational energy map for **1c** (Figure 9) shows isoenergetic global minima at $\phi_1 = \phi_2 \simeq 60°$ (for the *P*-chirality enantiomer) and at ($\phi_1 = \phi_2 \simeq -60°$), ($\phi_1 \simeq 300°$, $\phi_2 \simeq -60°$), ($\phi_1 \simeq -60°$, $\phi_2 \simeq 300°$), and ($\phi_1 \simeq \phi_2 \simeq 300°$) (for the *M*-chirality enantiomer). These global minima (corresponding to the lower structures of Figure 4) lie ~2 kcal/mol above the global minimum of *M*-chirality **1a** (Figure 4, upper left) (or *P*-chirality **1b**), and the lowest energy interconversion barriers are predicted to be close to those of bilirubin (Figure 2) or mesobilirubin XIIIα. These data strongly support the intramolecularly hydrogen-bonded conformations of Figure 4 (lower), wherein one β-CH_3 is located in a nonhindered site and the other β-CH_3 is sterically compressed into the C-10 –CH_2–.

The clear distinctions found in $CDCl_3$ for the ^{1}H-NMR spectra of **1c** and (**1a** + **1b**) are lost in $(CD_3)_2SO$ solvent. The expected changes in CO_2H and N–*H* chemical shifts are found and have been ascribed previously to a change from CO_2H to dipyrrinone intramolecular hydrogen bonding (in $CDCl_3$) to $(CD_3)_2SO$ hydrogen bonding to dipyrrinone and CO_2H units.[5,8,9,12] The resulting conformation is believed to be one where the propionic acid groups are tied to the dipyrrinones through $(CH_3)_2SO$ solvent.[11,12] We assume that in $(CH_3)_2SO$ the stable conformation retains a dissymmetry due to M and P type chirality, mutatis mutandis, because the pivotal C-10 –CH_2– hydrogens are nonequivalent in **1c**. Taken collectively, these results are consistent with the model of Figure 4 (right), a minimum energy structure for **1c** which is desymmetrized by failure of both halves to hydrogen bond equally effectively in $CDCl_3$.

Stereochemistry, Conformational Analysis, and Circular Dichroism. As discussed earlier, conformational enantiomerism can be driven toward either side by external factors that displace the equilibrium, such as chiral complexation agents, including proteins[19] and optically active amines.[20,21] Alternatively, equilib-

(19) (a) For leading references see: Blauer, G. *Isr. J. Chem.* **1983**, *23*, 201–209. (b) Lightner, D. A.; Wijekoon, W. M. D.; Zhang, M.-H. *J. Biol. Chem.* **1988**, *263*, 16669–16676.

(20) (a) Lightner, D. A.; An, J.-Y.; Pu, Y.-M. *Arch. Biochem. Biophys.* **1988**, *262*, 543–559. (b) Pu, Y. M.; Lightner, D. A. *Croat. Chem. Acta* **1989**, *62*, 301–324.

(21) Lightner, D. A.; Gawroński, J. K.; Wijekoon, W. M. D. *J. Am. Chem. Soc.* **1987**, *109*, 6354–6362.

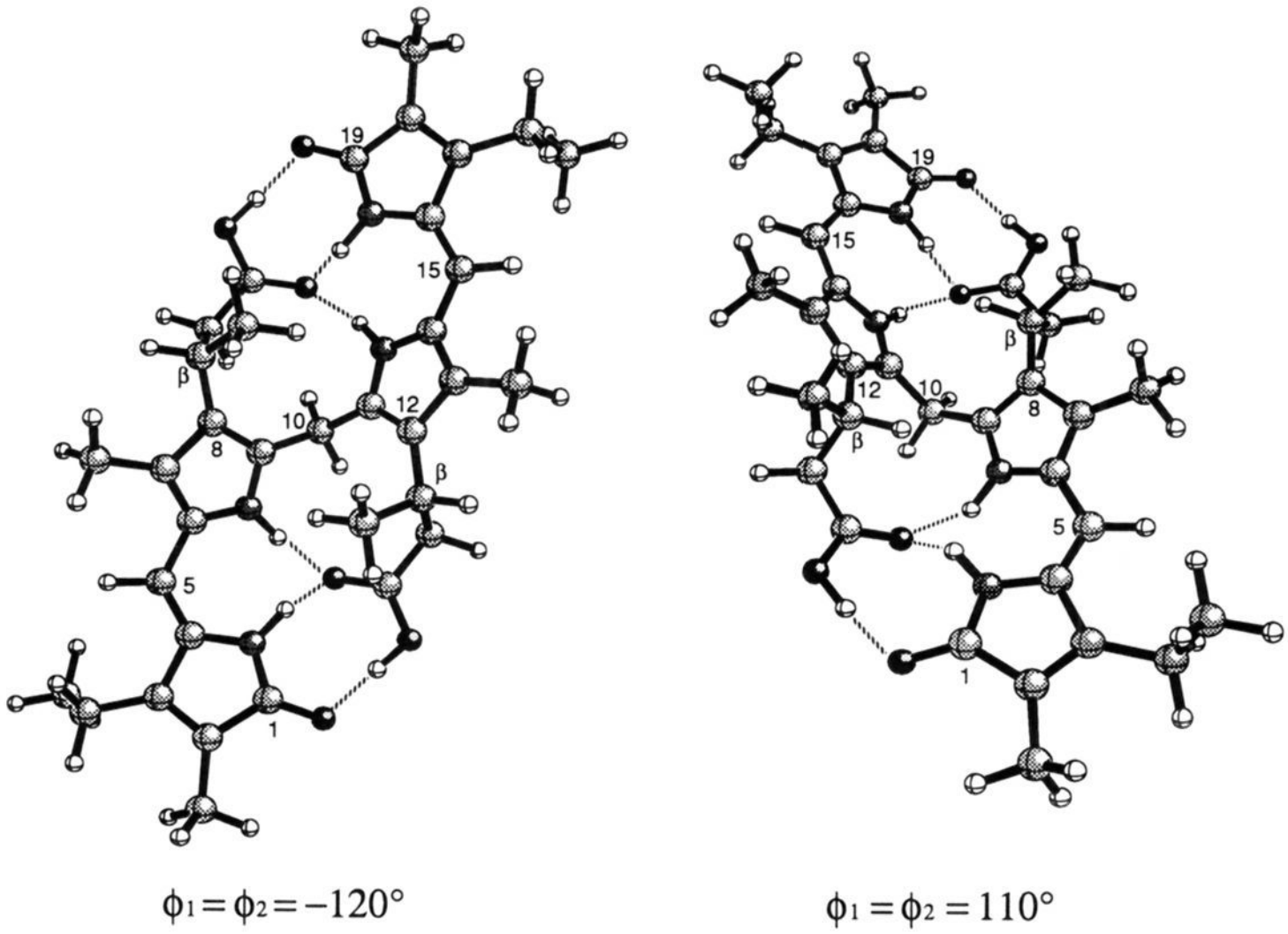

Figure 8. Ball and stick representations of ($\beta S,\beta' S$)-dimethylmesobilirubin XIIIα conformations at secondary local minima (see conformational energy map of Figure 7) located at $\phi_1 = \phi_2 \simeq -120°$ (left) and $\phi_1 = \phi_2 \simeq 110°$ (right). The conformation on the left is also identical to those at $\phi_1 = \phi_2 \simeq 240°$; $\phi_1 = -120°$, $\phi_2 = 240°$; and $\phi_1 = 240°$, $\phi_2 = -120°$ on Figure 7.

rium-displacing perturbations of an intramolecular origin can be induced by methyl substitution of the propionic side chain in the intramolecularly hydrogen-bonded pigment. In the current work, the β-methylated mesobilirubins serve as excellent chiral probes of pigment conformational stereochemistry. Thus, as seen above, when bilirubin or its symmetric analog, mesobilirubin XIIIα[21] (Figure 3) is folded and held in the *M*-chirality ridge-tile conformation by intramolecular hydrogen bonding, molecular models show that the *pro-R* β- and β'-hydrogens come in close contact with the C-10 $-CH_2-$ hydrogens whereas the *pro-S* hydrogens are in a sterically less crowded environment. In the *P*-helicity conformer, the inverse situation obtains, with the *pro-S* β- and β'-hydrogens being in the more sterically crowded environment. Consequently, replacement of the *pro-S* hydrogens by CH_3 groups can be expected to drive the conformational equilibrium strongly toward the *M*-chirality conformer, and replacement of the *pro-R* hydrogens should drive it toward the *P*-chirality conformer. However, in the absence of intramolecular hydrogen-bonded stabilization of the enantiomeric ridge-tile conformations, the intramolecular allosteric effect of methyl substitution would be lost and minimal conformational enantioselectivity would be expected.

If the predicted forced displacement of the $M \rightleftarrows P$ equilibrium is achieved through internal steric interactions introduced by the β,β'-CH_3 groups, then the pigment (**1a** or **1b**) can be expected to exhibit a special type of optical activity. One can expect modest optical activity due to some sort of $\pi-\pi^*$ excitation in the dipyrrinone perturbed by dissymmetric vicinal action from the β,β' asymmetric centers. But if the two dipyrrinones are held in a fixed relative geometry (*M* or *P*) through intramolecular hydrogen bonds and if the β,β'-methyl groups force a resolution to give *M* or *P*, depending on the *R,S* stereochemistry at β and β', then a strong exciton chirality interaction should lead to strong optical activity. Detection of optical activity (and an excess of the *M*- or *P*-chirality conformer) can be accomplished by circular dichroism (CD) spectroscopy (Figure 3) because these conformational enantiomers are predicted[21] to exhibit intense bisignate Cotton effects (CEs), with $|\Delta\epsilon|$ values computed to approach 270 $L \cdot mol^{-1} \cdot cm^{-1}$ for the pure enantiomers. CD spectra with two oppositely signed CEs straddling high-intensity UV–visible bands are typical of excited-state (electric dipole) interaction, or exciton coupling, between two proximal chromophores with little orbital overlap.[22,23] The component dipyrrinone chromophores of the bichromophoric mesobilirubin have strongly allowed long-wavelength electronic transitions ($\epsilon_{410}^{max} \sim 37{,}000$) but only a small interchromophoric orbital overlap in the folded conformation (where the dihedral angle $\simeq 100°$). They interact through resonance splitting, i.e., by electrostatic interaction of the local transition moment dipoles, which are oriented along the long axis of each dipyrrinone.[4,24] The dipyrrinone–dipyrrinone intramolecular exciton splitting interaction produces two long-wavelength transitions in the ordinary (UV–visible) spectrum and two corresponding bands in the CD spectrum.[21] One band is higher in energy and one is lower in energy, with the separation dependent on the strength and relative orientation of the dipyrrinone electric dipole transition moments.[25] When observed by UV–visible spectroscopy, the two electronic transitions overlap to give the broadened long-wavelength absorption band characteristic of bilirubins. In the CD spectra, however, where the two exciton transitions are oppositely signed, as predicted by theory,[21,23] bisignate CEs are typically seen. Thus, in contrast to the case of UV–visible absorption bands, which may show only slight broadening when the exciton splitting energy is small,[26] when two oppositely signed curves overlap in the CD, there is considerable cancellation in the region between the band centers with the net result that the *observed* bisignate CE maxima are displaced from the actual locations of the (uncombined) CD transitions which typically flank the corresponding UV–visible band(s).[19b,20,21,23] Typically bilirubin-like exciton-splitting CD

(22) Trull, F. R.; Franklin, R. W.; Lightner, D. A. *J. Heterocycl. Chem.* **1987**, *24*, 1573–1579.
(23) Harada, N.; Nakanishi, K. *Circular Dichroic Spectroscopy-Exciton Coupling in Organic Stereochemistry*; University Science Books: Mill Valley, CA, 1983.
(24) Lightner, D. A.; Reisinger, M.; Wijekoon, W. M. D. *J. Org. Chem.* **1987**, *52*, 5391–5395.
(25) Blauer, G.; Wagnière, G. *J. Am. Chem. Soc.* **1975**, *97*, 1949–1954.

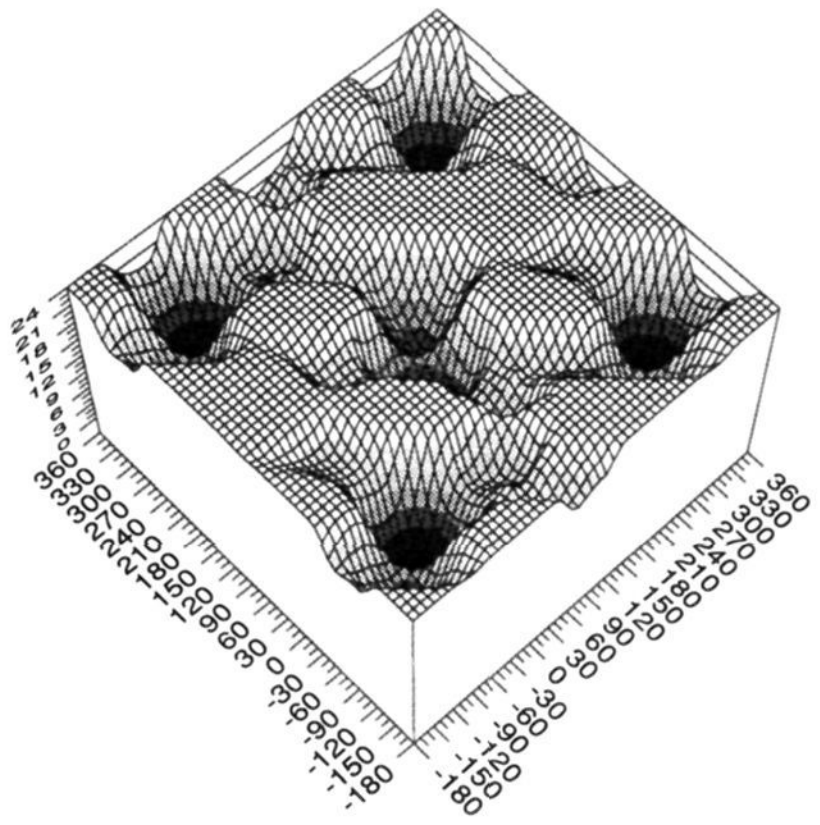

Figure 9. (Upper) Potential energy surface and (lower) contour maps for ($\beta S,\beta R$)-dimethylmesobilirubin XIIIα conformations generated by rotating the two dipyrrinone groups independently about the C-9–C-10 and C-10–C-11 bonds (ϕ_1 and ϕ_2, respectively). The energy scale (bottom) is in kcal/mol, and global minima (set to 0 kcal/mol) are found near (ϕ_1,ϕ_2) = (60°,60°) (*P*-helicity) and (ϕ_1,ϕ_2) = (−60°,−60°), (−60°,300°), (300°,−60°), and (300°,300°) (*M*-helicity). Data are from molecular dynamics simulations using SYBYL (Tripos Associates) on an Evans & Sutherland ESV-10 workstation.

spectra are illustrated by the spectra shown in Figure 10.

In complete agreement with the predictions of the allosteric model and exciton-coupling theory,[21] as shown in Table II, the *S,S* enantiomer of β,β'-dimethylmesobilirubin XIIIα (**1a**) shows an intense bisignate CD that is characteristic of the *M*-helicity conformational enantiomer, and the *R,R* enantiomer (**1b**) shows

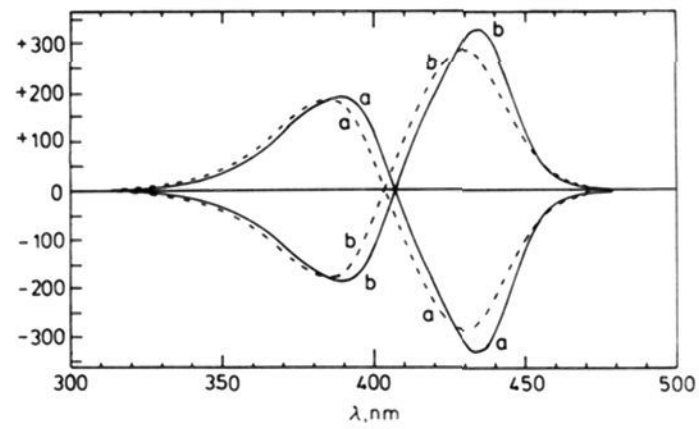

Figure 10. Circular dichroism spectra of 1.2×10^{-5} M solutions of (−)-$\beta S,\beta' S$-dimethylmesobilirubin XIIIα (a) and (+)-$\beta R,\beta' R$-dimethylmesobilirubin XIIIα (b) in $CHCl_3$ (solid line) and CH_3OH (dashed line) solvents at 22 °C. The $\Delta\epsilon^{max}$ (λ^{max}) values are −337 (434) and +186 (390) in $CHCl_3$ and −285 (431) and +177 (385) in CH_3OH for enantiomerically pure **1a**, with the corresponding, oppositely signed $\Delta\epsilon^{max}$ values for **1b**.

an equally intense bisignate CD characteristic of the *P*-helicity conformer. In Figure 10, attention is drawn to the fact that in shifting from a nonpolar solvent to a polar, hydroxylic solvent, the CD intensity is only slightly decreased, implying nearly the same enantioselectivity in both solvents and very little loosening or disruption of the intramolecular hydrogen-bonding network. The $\Delta\epsilon$ values in nonpolar solvents like $CHCl_3$ ($\Delta\epsilon^{max}_{434}$ −337, $\Delta\epsilon^{max}_{390}$ +186) are close to the theoretically predicted maximum values[19] and not very different from the average $|\Delta\epsilon|$ values taken over a wide range of organic solvents (except $(CH_3)_2SO$): 183 for the short-wavelength component and 324 for the long-wavelength component. Thus, although one might expect the intramolecular hydrogen bonding (which is so very important in stabilizing the *M*-chirality conformation of **1a** and the *P*-chirality conformation of **1b**) to be strongest in nonpolar solvents such as chloroform or diethyl ether and weaker in polar aprotic solvents such as acetonitrile or acetone, the CD intensities in these solvents are within 10% of the average $|\Delta\epsilon|$ values. Apparently, there is very little influence from the polar solvent in disrupting the intramolecular hydrogen-bonding network.

Surprisingly, even in polar, hydroxylic organic solvents such as ethanol or methanol, the $\Delta\epsilon$ values are not significantly reduced from the $\Delta\epsilon$ values of nonpolar or other polar solvents. In basified water, the CD magnitudes still remain quite large, although only about half of the average value for the organic solvents. Whether the greater loss of *M* vs *P* conformational selectivity is due to ionization of the carboxylic acid groups or to the large dielectric constant or to the greater hydrogen-bonding ability of water is unclear. However, previous work has shown that deprotonation of the carboxyl hydrogen does not necessarily lead to substantial disruption of the network intramolecular hydrogen bonds, as the strength of the remaining hydrogen bonds (to the carboxylate ion) is intensified.[19b,20] The very large $\Delta\epsilon$ values in alkaline pH water support the presence (probably a major presence) of folded intramolecularly hydrogen-bonded conformations in bilirubincarboxylate anions. These observations are of considerable importance to studies of bilirubin in biological systems and in studies of its metabolism.

The CD in $(CH_3)_2SO$ is the major exception. Not only are the CD magnitudes reduced to only 3–7% of the average $|\Delta\epsilon|$ values but the Cotton effect signs are also inverted. $(CH_3)_2SO$ is known to be a potent hydrogen bond acceptor[5,8] and is thought to coordinate to the dipyrrinone N–*H*s by disrupting the conventional intramolecular hydrogen-bonding matrix (Figure 3) and replacing it with a matrix of hydrogen bonds wherein the propionic acid carboxyls are linked to the dipyrrinones through $(CH_3)_2SO$ solvent.[9,10b,11,12] In this model, where intramolecular hydrogen bonding is swollen through solvent participation, the allosteric effects due to the β,β'-methyls are apparently substantially decreased and play only a limited role in the selection of the most stable conformational diastereomer. Consequently, solutions of bilirubin in $(CH_3)_2SO$ are probably not good models for solutions

(26) Kasha, M.; Rawls, H. R.; El-Bayoumi, M. A. *Pure Appl. Chem.* **1965**, *11*, 371–392.

(27) Motherwell, W. D. S.; Clegg, W. PLUTO78: A program for drawing crystal and molecular structures. University of Cambridge, England, 1978.

Table II. Circular Dichroism and Ultraviolet–Visible Spectral Data from 5×10^{-5} M ($\beta S,\beta' S$)-Dimethylmesobilirubin XIIIα (**1a**) and ($\beta R,\beta' R$)-Dimethylmesobilirubin XIIIα (**1b**) at 22 °C

			CD			UV	
enantiomer	solvent	dielectric constant[a]	$\Delta\epsilon^{max}$ (λ_1 in nm)	λ_2 at $\Delta\epsilon = 0$ (nm)	$\Delta\epsilon^{max}$ (λ_3, in nm)	ϵ^{max}	λ (nm)
1a	carbon tetrachloride	2.2	+179 (392)	406	−393 (434)	59 000	435
1b			−176 (392)	406	+385 (434)	60 800	435
1a	dioxane	2.2	+184 (389)	405	−336 (433)	56 600	431
1b			−180 (389)	405	+329 (433)	58 300	431
1a	benzene	2.3	+191 (390)	406	−362 (434)	55 400	433
1b			−204 (391)	407	+380 (434)	60 000	432
1a	toluene	2.4	+196 (391)	406	−375 (434)	55 800	433
1b			−192 (391)	406	+367 (434)	57 500	433
1a	diethyl ether	4.3	+183 (387)	402	−365 (429)	57 500	429
1b			−179 (387)	402	+357 (429)	59 200	429
1a	chloroform	4.7	+186 (389)	407	−337 (434)	55 500	431
1b			−188 (389)	407	+332 (435)	55 800	431
1a	tetrahydrofuran	7.3	+188 (390)	406	−338 (433)	56 200	431
1b			−184 (390)	406	+331 (434)	57 900	431
1a	dichloromethane	8.9	+180 (392)	407	−319 (433)	54 800	430
1b			−176 (392)	407	+312 (433)	56 400	430
1a	1,2-dichloroethane	10.4	+193 (389)	407	−332 (433)	55 400	430
1b			−189 (389)	407	+325 (433)	57 100	430
1a	1-butanol	17.1	+181 (391)	408	−293 (435)	55 800	427
1b			−177 (391)	408	+287 (435)	57 500	427
1a	acetonitrile	36.2	+181 (384)	403	−315 (429)	55 000	423
1b			−177 (384)	403	+308 (429)	56 700	423
1a	1-propanol	20.1	+169 (388)	406	−253 (431)	55 900	426
1b			−165 (388)	406	+248 (431)	57 600	426
1a	acetone	20.7	+182 (387)	404	−322 (430)	55 400	426
1b			−178 (387)	404	+315 (430)	57 100	427
1a	ethanol	24.3	+168 (389)	405	−284 (434)	55 900	426
1b			−164 (389)	405	+278 (434)	57 600	426
1a	methanol	32.6	+177 (386)	405	−285 (431)	56 600	425
1b			−175 (386)	405	+269 (431)	60 800	425
1a	*N*,*N*-dimethylformamide	36.7	+165 (386)	404	−246 (429)	53 100	421
1b			−169 (386)	404	+252 (429)	54 000	421
1a	dimethylsulfoxide	46.5	−5.8 (369)	385	+23.0 (425)	55 900	425
1b			+4.3 (368)	384	−24.2 (422)	56 700	425
1a	borate buffer, pH 8.5–10.0	(78)[b]	+107 (379)	397	−171 (424)	51 900	418
1b			−105 (379)	397	+167 (424)	53 500	418
1a	phosphate buffer, pH 7.4	(78)[b]	+95 (379)	398	−150 (423)	44 500	416
1b			−93 (379)	398	+147 (423)	45 800	416
1a	*N*-methylformamide	182.4	+200 (383)	400	−359 (427)	66 000	426
1b			−188 (383)	405	+337 (427)	68 300	427

[a] From: Gordon, A. J.; Ford, R. A. *The Chemist's Companion*; Wiley, New York, 1972; pp 4–8. [b] Pure water.

of bilirubin in alkaline aqueous solvents or in biological systems.[13]

Concluding Comments

Through intramolecular allosteric action, ($\beta S,\beta' S$)-dimethylmesobilirubin XIIIα (**1a**), with absolute stereochemistry at the β-positions of the propionic acid groups determined by X-ray crystallography, is forced to adopt the *M*-helicity ridge-tile conformation in $CHCl_3$, in other nonpolar solvents, and even in polar, hydroxylic solvents. Consistent with predictions, the *M*-helicity conformer exhibits intense bisignate negative exciton chirality circular dichroism for the long-wavelength transition(s), with the CD intensity dropping by only 15% in going from nonpolar solvents such as chloroform or benzene to more polar solvents such as acetonitrile or even polar, hydroxylic solvents such as methanol. Even in alkaline pH water, the CD intensities remain very high. These findings are important because (1) they establish the importance of intramolecular hydrogen bonding and how it can be used to control the handedness of conformations and (2) they firmly establish that the *M*-helicity conformational enantiomer of bilirubin will exhibit a negative exciton chirality CD.

Experimental Part

General Methods. Circular dichroism spectra were run on a JASCO J-600 spectropolarimeter, and UV–visible spectra were recorded on a Cary 219 or Perkin-Elmer 3840 diode array instrument. Rotations were determined on a Perkin-Elmer Model 141 polarimeter. Nuclear magnetic resonance (NMR) spectra were recorded on a GE QE-300 or GN-300 300-MHz instrument, and infrared (IR) spectra were measured on a Perkin-Elmer Model 1610 FT instrument. HPLC analyses were carried out on a Perkin-Elmer high-pressure liquid chromatograph with an LC-95 UV–vis spectrophotometric detector (set at 410 nm) equipped with a Beckman-Altex ultrasphere-IP 5-μm C-18 ODS column (25 × 0.46 cm) and Beckman ODS precolumn (4.5 × 0.46 cm). The flow rate was 2.0 mL·min.$^{-1}$. The eluting solvent was 0.1 M di-*n*-octylamine acetate in 5% aqueous methanol (pH 7.7 at 31 °C). Melting points were determined on a Mel-Temp capillary apparatus and are uncorrected. Combustion analyses were carried out at Desert Analytics, Tucson, Arizona.

Spectral data were obtained in spectral grade solvents (Aldrich or Fisher). Pentane-2,4-dione, ethyl acetoacetate, methyl crotonate, diethylene glycol, dimethyl sulfoxide, tetrahydrofuran, formic acid, and *p*-chloranil (tetrachloro-1,4-benzoquinone) were from Aldrich. Methanol, 2-propanol, dichloromethane, and chloroform were HPLC grade from Fisher; hydrogen peroxide and zinc dust were from Fisher. Tetrahydrofuran was dried by distillation from $LiAlH_4$; methanol was dried (Mg, reflux) and distilled. Brucine ($[\alpha]^{20}_D$ −79°) was used as obtained from Sigma.

X-Ray Crystallography. Diffraction measurements were made at 25 °C on a colorless crystal of the brucine salt of **5a**, grown from a solution in acetone and mounted on a Huber diffractometer constructed by C. E. Strouse. The crystal is monoclinic, space group $P2_1$. Precise cell dimensions were determined with Mo Kα radiation, from a least-squares fit to 23 reflections ($7.6° < 2\theta < 19.9°$): a = 8.170 (1), b = 12.383 (1), c = 18.945 (1) Å; β = 95.52 (1)°; V = 1908 Å^3; Z = 2. There were 5803 unique reflections (to $2\theta_{max} = 60°$), of which 2734 had $I > 2\sigma(I)$; the latter were used in solving the structure by direct methods (SHELX86[28a]) and refining by least squares (SHELX76[28b]). All calculations were made on a VAX3100 computer in the James D. McCullough X-Ray Crystallography Laboratory at UCLA. All non-H atoms were found by direct methods; H atoms were found on difference Fourier maps. The $\langle u^2 \rangle$ for

each H atom was based approximately on the corresponding value for the attached atom. Anisotropic displacement parameters were refined for all non-H atoms of the anion, for all non-H solvent atoms, and for all O atoms of the cation. All H bonded to C were refined as riding or as parts of rigid groups, C–H = 1.08 Å; H bonded to O and N were kept at the positions at which they were located. Scattering factors were taken from the International Tables for X-Ray Crystallography.[29] The final R-value was 0.071 (R_W = 0.072); the height of the largest peak in the final difference map was 0.2 e·Å^{-3}.

5-(Bromomethylene)-4-ethyl-3-methyl-2-oxo-1*H*-pyrrole (7). This synthetic relay component was prepared in four steps from ethyl acetoacetate and pentane-2,4-dione as described previously.[14] It had mp 137–139 °C [lit.[16] mp 138–140 °C]; IR (KBr) 3353, 3107, 2967, 1699, 1640 cm^{-1}; ^{1}H-NMR ($CDCl_3$) δ 1.14 (t, 3 H, J = 7.5 Hz), 1.86 (s, 3 H), 2.42 (q, 2 H, J = 7.5 Hz), 5.92 (s, 1 H), 7.30 (br s, 1 H) ppm; ^{13}C-NMR ($CDCl_3$) δ 8.35 (q), 14.20 (q), 17.90 (t), 86.93 (d), 129.59 (s), 141.30 (s), 145.28 (s), 171.33 (s) ppm.

Methyl 3-[2,4-Dimethyl-5-(ethoxycarbonyl)-1*H*-pyrrol-3-yl]butanoate (6). Methyl crotonate (400 g, 4.0 mol) was mixed with pentane-2,4-dione (400 g, 4.0 mol) and diluted with 700 mL of 2-propanol. To this solution was added potassium fluoride dihydrate (188 g, 2.0 mol) (previously pulverized in a mortar), and the mixture was heated at reflux for 5 days with stirring. The mixture was kept overnight at 0 °C, and the potassium fluoride was removed by filtration and washed with CH_2Cl_2. To the filtrate was added 1 L of water, and the product was extracted into CH_2Cl_2 (4 × 250 mL). After the organic layers were dried over anhydrous $MgSO_4$ and filtered and solvent was removed (rotovap), the residue was distilled under vacuum to afford 328 g (41%) of purified product (methyl 4-acetyl-3-methyl-5-oxohexanoate), bp 118–126 °C (3 mm Hg). It had IR (neat) 1730, 1698 cm^{-1}; ^{1}H-NMR ($CDCl_3$) δ 1.15 (t, 3 H, J = 7 Hz), 2.09 and 2.12 (s, 3 H, enol and keto CH_3), 1.80–2.60 (m, 3 H, $-CH_2-$ and $-CH-$), 3.60 (s, 3 H, OCH_3), 3.70 (t, 1 H, J = 7.5 Hz), 16.85 (s, 1 H, enol OH). The material was used directly in the following step.

Ethyl acetoacetate (156.0 g, 1.20 mol) was dissolved in 420 mL of glacial acetic acid and treated dropwise with a solution of sodium nitrite (117.3 g, 1.70 mol) in 180 mL of water at a rate so that the temperature did not exceed 10 °C while maintaining efficient stirring. The solution was stirred at room temperature overnight, and then the hexanoate ester above (120 g, 0.60 mol) was added in one dose followed by the addition of 100 mL of glacial acetic acid and zinc dust (186 g, 2.83 g·atoms) in small portions to maintain the reaction temperature at 65 °C. After the final addition, the reaction mixture was heated at reflux for 36 h and then poured onto 6 L of ice and water. The solidified product was filtered and dissolved into 600 mL of $CHCl_3$. Nonsoluble inorganic materials were removed by filtration, and the filtrate was washed with 2 × 200 mL of water and dried over anhydrous $MgSO_4$. After evaporation of the solvent, the residue was diluted with 40 mL of 85% ethanol and the product crystallized at −20 °C (4 days). It was removed by filtration and washed with cold 85% ethanol to give 36.55 g (23%) of pure pyrrole (±)-**6**, mp 92–93.5 °C. It had IR (film) 3312, 2965, 2932, 2874, 1736, 1662 cm^{-1}; ^{1}H-NMR ($CDCl_3$) δ 1.23 (d, 3 H, J = 6.9 Hz), 1.32 (t, 3 H, J = 7 Hz), 2.23 (s, 3 H), 2.32 (s, 3 H), 2.58 (d, 2 H, J = 7.1 Hz), 3.27 (tq, 1 H, J = 7.1, 6.9 Hz), 3.59 (s, 3 H, OCH_3), 4.26 (q, 2 H, J = 7 Hz), 8.50 (br s, 1 H, NH) ppm; ^{1}H-NMR (benzene-d_6) δ 1.03 (t, 3 H, J = 7.5 Hz), 1.17 (d, 3 H, J = 6.9 Hz), 1.78 (s, 3 H), 2.49 (2 × dd, 2 H, J_{AB} = 15 Hz, J_{AX} = 7.4 Hz, J_{BX} = 8.3 Hz), 2.52 (s, 3 H), 3.25 (s, 3 H), 3.37 (m, 1 H), 4.13 (q, 2 H, J = 7.5 Hz), 8.63 (br s, 1 H) ppm; 2.52 (s, 3 H), 3.25 (s, 3 H), 3.37 (m, 1 H), 4.13 (q, 2 H, J = 7.5 Hz), 8.63 (br s, 1 H) ppm; ^{13}C-NMR ($CDCl_3$) δ 11.0 (q), 12.4 (q), 14.5 (q), 20.3 (q), 27.5 (d), 41.0 (t), 51.3 (q), 59.6 (t), 116.9 (s), 124.2 (s), 126.5 (s), 129.3 (s), 161.8 (s), 173.1 (s) ppm. Anal. Calcd for $C_{14}H_{21}NO_4$ (267.3): C, 62.90; H, 7.92; N, 5.24. Found: C, 63.07; H, 8.09; N, 5.16

(±)-3-[2,4-Dimethyl-5-(ethoxycarbonyl)-1*H*-pyrrol-3-yl]butanoic Acid (5). To a solution of 26.73 g (0.1 mol) of **6** in 250 mL of ethanol was added a solution of 4.0 g (0.1 mol) of sodium hydroxide in 40 mL of water, and the mixture was stirred at room temperature for 20 h. After evaporation of the ethanol, to the residue was added 0.2 M aqueous solution of sodium hydroxide (300 mL) and neutral organics were extracted with 2 × 100 mL of chloroform. The water layer was partially evaporated in vacuum to remove traces of chloroform and was carefully acidified with 10% HCl at 3 °C with vigorous stirring. The solid product was filtered, washed with water until the filtrate was neutral, and dried in vacuum to give 23.05 g (91%) (±)-**5**, mp 154–155.5 °C. It had IR (KBr pellet) 3304, 2990, 2960, 2923, 1697, 1659, 1569, 1502, 1442 cm^{-1}; ^{1}H-NMR ($CDCl_3$) δ 1.29 (d, 3 H, J = 7.0 Hz), 1.34 (t, 3 H, J = 6.9 Hz), 2.20 (s, 3 H), 2.34 (s, 3 H), 2.63 (d, 2 H, J = 7.0 Hz), 3.29 (q, 1 H, J = 7.1 Hz), 4.29 (q, 2 H, J = 6.9 Hz), 8.82 (br s, 1 H, NH), ~11 (very broad, COOH) ppm; ^{13}C-NMR ($CDCl_3$) δ 11.2 (q), 12.3 (q), 14.6 (q), 20.4 (q), 27.5 (t), 40.9 (d), 59.8 (t), 116.9 (s), 123.8 (s), 126.8 (s), 129.6 (s), 162.1 (s), 177.6 (s) ppm.

Table III. Optical Rotations $[\alpha]^{20}_D$ (c 0.8–1.6, C_2H_5OH) of the Fractions during Resolution of Pyrrole Acid **5**

		corresponding free acid from	
fraction no.	brucine salt	crystalline salt	mother liquor
1	−21.6	+5.6	−14.1
2	−15.2	+25.3	−19.0
3	−15.5	+30.5	+14.5
4	−14.8	+30.8	+24.7

Resolution of (±)-3-[2,4-Dimethyl-5-(ethoxycarbonyl)-1*H*-pyrrol-3-yl]butanoic Acid. 25.33 g (0.1 mol) of the acid (±)-**5** and 43.05 g (0.1 mol) of (−)-brucine dihydrate were mixed and dissolved at reflux in 550 mL of acetone. After 24 h at room temperature and overnight at 0 °C, 42.60 g of crystalline brucine salt were filtered. Three recrystallizations of this salt from acetone (ratio salt (g):acetone (mL) = 1:7) led to 19.37 g of salt, mp 94–96 °C dec, with $[\alpha]^{20}_D$ = −15.1° (c 1.1, ethanol) (Table III). The optical rotations for the salt and the free acid (+)-**5** were the same after additional recrystallization of the salt from acetone. After recrystallization of the above salt (0.3 g from 10 mL of acetone) several monocrystals were obtained suitable for X-ray analysis.

The salt (+)-**5**–(−)-brucine (19.3 g) was dissolved in 50 mL of methanol and acidified with diluted HCl. Water (~200 mL) was added dropwise to crystallize completely the free acid, which after 24 h at 0 °C was filtered off, washed with water, and dried in vacuum to give 6.23 g (+)-**51** (49% of the enantiomer), mp 148–150 °C, $[\alpha]^{20}_D$ = +30.5° (c 0.8, ethanol).

(±)-Methyl 3-[2,7,9-Trimethyl-3-ethyl-1-oxo-1,10-dihydrodipyrrin-8-yl]butanoate (3). Diester **6** (5.3 g, 19.8 mmol) was saponified to the diacid by heating at reflux for 2 h in a solution of sodium hydroxide (4.00 g, 100 mmol) in 40 mL of 96% ethanol containing 15 mL of 50% aqueous sodium nitrate. The ethanol was removed on a rotary evaporator; then the residue was cooled to −15 to −10 °C, and the nonhomogeneous mixture was acidified with 65 mL of a solution of nitric acid–50% aqueous $NaNO_3$ (1:5 vol/vol), added dropwise and with mechanical stirring to precipitate the diacid (**4**). The product was collected by filtration, washed carefully with ice water (250 mL), and dried in a vacuum desiccator over phosphorus pentoxide to give 3.86 g (86%) of pure diacid (**4**), which had IR (KBr pellet) 3330, 2943, 2605, 1899, 1667, 1506, 1454 cm^{-1}; ^{1}H-NMR ($(CD_3)_2SO$) δ 1.12 (d, 3 H), 2.11 (s, 3 H), 2.18 (s, 3 H), 2.41 (octet, 2 H), 3.08 (hextet, 1 H), 10.85 (br s, 1 H), 11.85 (br s, 2 H) ppm; ^{13}C-NMR ($(CD_3)_2SO$) δ 11.1 (q), 12.2 (q), 20.7 (q), 27.3 (t), 41.3 (d), 116.6 (s), 123.7 (s), 125.3 (s), 129.4 (s), 162.7 (s), 173.9 (s) ppm. It was used directly in the next step.

The diacid (3.86 g, 17 mmol) and 3.67 g (17 mmol) of the (bromomethylene)oxopyrrole (**7**) were dissolved in 85 mL of methanol plus 1 mL of water, and the resulting solution was purged with nitrogen and heated at mild reflux with stirring for 6 h, during which the yellow dipyrrinone precipitated. The reaction mixture was cooled overnight at −20 °C, and the product was removed by filtration and washed thoroughly with cold methanol. Traces of (unesterified) free acid could be removed by chromatography on a column of silica gel (CH_2Cl_2–CH_3OH, 100:1 vol/vol, elutes the ester), and the desired dipyrrinone ester was recrystallized from benzene–hexane 2:1 to give 3.5 g (60%) of the bright yellow product, mp 209–211 °C. It had IR (film) 3351, 2964, 2922, 2872, 1738, 1667, 1633 cm^{-1}; UV–vis ϵ^{max}_{408} 35 900, ϵ^{max}_{265} 4560 ($CHCl_3$), ϵ^{max}_{412} 36 700, ϵ^{max}_{266} 4800 (CH_3OH), ϵ^{max}_{417} 33 500 ($(CH_3)_2SO$); ^{1}H-NMR ($CDCl_3$) δ 1.17 (t, 3 H, J = 7.5 Hz), 1.29 (d, 3 H, J = 7.2 Hz), 1.94 (s, 3 H), 2.19 (s, 3 H), 2.47 (s, 3 H), 2.54 (q, 2 H, J = 7.6 Hz), 2.62 (d, 2 H, J = 7.7 Hz), 3.33 (hextet, 1 H, J = 7.5 Hz), 3.63 (s, 3 H), 6.13 (s, 1 H), 10.30 (br s, 1 H), 11.30 (br s, 1 H) ppm; ^{13}C-NMR ($CDCl_3$) δ 8.5 (q, C-10), 10.2 (q, C-2^1), 12.6 (q, C-7^1), 15.0 (q, C-3^2), 17.9 (t, C-3^1), 20.4 (q, C-8^4), 27.6 (d, C-8^1), 41.1 (t, C-8^2), 51.4 (q, OCH_3), 100.9 (d, C-5), 122.2 (s, C-7), 122.3 (s, C-8), 123.3 (s, C-6), 124.1 (s, C-2), 127.1 (s, C-4), 131.0 (s, C-9), 148.4 (s, C-3), 173.2 (s, C-1), 174.1 (s, C-8^3) ppm; see Table I for numbering system. Anal. Calcd for $C_{19}H_{26}N_2O_3$ (330.4): C, 69.07; H, 7.93; N, 8.48. Found: C, 68.99; H, 8.01; N, 8.52.

(+)-(*S*)-Methyl 3-[2,7,9-Trimethyl-3-ethyl-1-oxo-1,10-dihydrodipyrrin-8-yl]butanoate (3a). Monoester **5a** (3.29 g, 13 mmol) with $[\alpha]^{20}_D$ = +30.5° (c 0.8, ethanol) was converted to diacid **4a** by refluxing in 25 mL of ethanol and 10 mL of 50% aqueous $NaNO_3$ with 2.60 g (65

(28) (a) Sheldrick, G. M. *Acta Crystallogr.* **1990**, *A46*, 467–473. (b) Sheldrick, G. M. Program for crystal structure determination. University of Cambridge, England, 1976.

(29) Ibers, J. A.; Hamilton, W. C., Eds. *International Tables for X-Ray Crystallography*; Kynoch Press: Birmingham, England, 1974; Vol. IV, p 99.

mmol) of sodium hydroxide for 2 h. After evaporation of the ethanol, the product was precipitated at −15 to −10 °C with 40 mL of a 1:5 solution of concentrated HNO_3–50% aqueous $NaNO_3$. The diacid **4a** was filtered off, washed with ice water, dried in vacuum, and used in the next step.

Diacid **4a** (2.80 g, 12 mmol) and (bromomethylene)oxopyrrole **7** (2.68 g, 12 mmol) were dissolved in 60 mL of methanol, and the resulting mixture was refluxed for 9 h under nitrogen. The reaction mixture was cooled at −20 °C overnight, and the product was filtered off, washed with cold methanol, and recrystallized from dichloromethane–methanol = 1:4, yielding 2.14 g of **3a** (50% for both stages) mp 207–210 °C dec, $[\alpha]^{20}_D$ = +61.8° (*c* 0.8, chloroform).

(−)-(*R*)-Methyl 3-[2,7,9-Trimethyl-3-ethyl-1-oxo-1,10-dihydrodipyrrin-8-yl]butanoate (3b). Monoester **5b** (2.31 g, 9.1 mmol) with $[\alpha]^{20}_D$ = −24.4° (*c* 1.3, ethanol), 80% ee, was converted to diacid **4b** and on to **3b** as described above for the *S* enantiomer. The yield of **3b** was 1.04 g (34% for both stages), mp 210–214 °C dec, $[\alpha]^{20}_D$ = −51.2° (*c* 0.8, $CHCl_3$).

β,β′-Dimethylmesobiliverdin XIIIα Dimethyl Ester (2). To a refluxing mixture of 1.23 g (5 mmol) of *p*-chloranil in 300 mL of dichloromethane was added a solution of 661 mg (2 mmol) of dipyrrinone (±)-**3** in 150 mL of dichloromethane, followed by 20 mL of 97% formic acid. The mixture was heated at reflux for 18 h. Then 200 mL of solvent was removed by distillation, and reflux was continued for an additional 24 h. The reaction mixture was kept overnight at −20 °C, filtered, washed with cold (2 × 50 mL) dichloromethane, and carefully neutralized in the cold with 10% aqueous $NaHCO_3$, added portionwise. The dichloromethane solution was consecutively washed with 3 × 150 mL of 1 M NaOH and 3 × 300 mL of water. After the organic layer was dried over anhydrous $MgSO_4$ and filtered and the solvent was removed (rotovap), the crude product was purified by column chromatography on silica gel. Elution with 2% methanol in dichloromethane yielded 459 mg (71%) of **2**, mp 225–227 °C. It had UV ($CHCl_3$) ϵ^{max}_{642} 13 500, ϵ^{max}_{368} 47 700, (CH_3OH), ϵ^{max}_{644} 12 500, ϵ^{max}_{363} 47 900, ($(CH_3)_2SO$), ϵ^{max}_{644} 13 100, ϵ^{max}_{371} 48 500; ^{1}H-NMR ($CDCl_3$) δ 1.20 (t, 6 H), 1.41 (d, 6 H), 1.79 (s, 6 H), 2.15 (s, 6 H), 2.50 (q, 4 H), 2.71 (d, 4 H), 3.52 (hextet, 2 H), 3.62 (s, 6 H), 5.95 (s, 2 H), 6.95 (s, 1 H), 8.06 (br s, 1 H) ppm; ^{13}C-NMR ($(CD_3)_2SO$) δ 8.3 (q), 9.7 (q), 14.5 (q), 17.9 (t), 26.5 (t), 41.0 (d), 49.5 (q), 51.8 (q), 93.9 (d), 111.6 (d), 125.5 (s), 125.6 (s), 133.7 (s), 136.9 (s), 138.6 (s), 143.8 (s), 146.8 (s), 149.9 (s), 172.4 (s), 176.4 (s) ppm. Anal. Calcd for $C_{37}H_{46}N_4O_6$ (642.8): C, 69.16; H, 7.17; N, 8.72. Found: C, 67.13; H, 6.95; N, 8.33. Calcd for $C_{37}H_{46}N_4O_6 \cdot H_2O$ (660.8): C, 67.25; H, 7.32; N, 8.48.

(−)-(βS,β′S)-Dimethylmesobiliverdin XIIIα Dimethyl Ester (2a). From 2.13 g (6.4 mmol) of **3a** and 3.97 g (16 mmol) of *p*-chloranil as described above for racemic **2** was obtained 1.54 g (74%) of optically active verdin **2a**, mp 208–214 °C, $[\alpha]^{20}_{436}$ = −2720° (*c* 0.0037, $CHCl_3$).

(+)-(βR,β′R)-Dimethylmesobiliverdin XIIIα Dimethyl Ester (2b). From 1.01 g (3 mmol) of **3b** (80% ee) and 1.88 g (7.5 mmol) of *p*-chloranil as described above for racemic **2** was obtained 0.77 g (80%) of optically active verdin **2b**, mp 208–214 °C.

β,β′-Dimethylmesobilirubin XIIIα (1). β,β′-Dimethylmesobiliverdin XIIIα dimethyl ester (**2**) (643 mg, 1 mmol) was dissolved in 350 mL of a 1:1 vol/vol mixture of tetrahydrofuran–methanol that had been purged with argon. Ascorbic acid (320 mg) was added followed by 350 mL of 0.2 M aqueous sodium hydroxide. The resulting blue solution was warmed to 45 °C and stirred for 4 h under argon. After cooling, the solution was transferred to a separatory funnel containing 50 mL of 0.2 M aqueous sodium hydroxide and washed with 100 mL of dichloromethane. The organic layer was discarded, and the blue aqueous layer was separated and acidified with 10% aqueous HCl and then extracted with dichloromethane (4 × 150 mL) to remove the verdin diacid, which was used in the reduction step without further purification.

In the following steps, it is important that all reactions, extractions, and chromatography be carried out under an argon or nitrogen atmosphere using argon- or nitrogen-saturated solvents. The verdin diacid (307 mg, 0.5 mmol) was dissolved in 100 mL of dry argon-saturated tetrahydrofuran. The solution was cooled in an ice bath, and 1.90 g (50 mmol) of sodium borohydride was added in one portion. After 10 min of stirring, 40 mL of dry argon-saturated methanol was added dropwise in a period of 20 min and stirring continued for 40 min. The reaction was quenched by addition of 50 mL of argon-saturated water. The pH of the mixture was adjusted to 2–3 by adding ~20 mL of cold 10% argon-saturated aqueous hydrochloric acid and an additional 100 mL of water. The rubin was extracted by dichloromethane (4 × 150 mL), and the combined extracts were washed with 50% saturated aqueous sodium bicarbonate so as to afford a bright yellow organic phase. The latter was dried over anhydrous sodium sulfate, filtered, and evaporated in vacuum to dryness. The crude product containing a 1:1 mixture of racemic (**1a** + **1b**)–meso (**1c**) diastereomers (by HPLC) was crystallized from dichloromethane–methanol ~1:2 v/v to give 217 mg (70%) rubins (**1a** + **1b**)–**1c** = 52:48. The mixture was successfully separated by column chromatography on 50 g of silica gel (deactivated with 7% water overnight) and eluted with argon-saturated chloroform. The separation was monitored by HPLC, and combined fractions containing each diastereomer were evaporated and recrystallized from dichloromethane–methanol ~1:2 v/v, leading to 110 mg of pure **1a** + **1b**, which is less polar on TLC, and 91 mg of **1c**, which is significantly more polar on TLC.

Racemic Diastereomer (1a + 1b): mp 290 °C dec; IR (KBr) 3412, 1686, 1250 cm^{-1}; UV–vis ϵ^{max}_{432} 56 200 ($CHCl_3$), ϵ^{max}_{426} 56 600 ($(CH_3)_2SO$), ϵ^{max}_{427} 62 500 (MeOH); ^{1}H-NMR in Table II; ^{13}C-NMR ($(CD_3)_2SO$) δ 8.09 (q, C-2^1, C-18^1), 10.65 (q, C-7^1, C-13^1), 14.86 (q, C-3^2, C-17^2), 17.18 (t, C-3^1, C-17^1), 19.84 (q, β,β′), 23.91 (t, C-10), 26.88 (d, C-8^1, C-12^1), 97.67 (d, C-5, C-15), 121.70 (s, C-8, C-12), 122.48 (s, C-6, C-14), 122.97 (s, C-2, C-18), 123.21 (s, C-7, C-13), 128.01 (s, C-9, C-11), 130.20 (s, C-4, C-16), 147.33 (s, C-3, C-17), 172.10 (s, C-8^3, C-12^3), 173.68 (s, C-1, C-19) ppm. Anal. Calcd for $C_{35}H_{44}N_4O_6$ (616.4): C, 68.16; H, 7.19; N, 9.08. Found: C, 67.39; H, 7.21; N, 8.90. Calcd for $C_{35}H_{44}N_4O_6 \cdot {}^1/_2H_2O$ (625.7): C, 67.19; H, 7.25; N, 8.95.

Meso Diastereomer (1c): mp 245 °C dec; IR (KBr) 3411, 1665, 1272 cm^{-1}; ^{1}H-NMR in Table II; ^{13}C-NMR ($(CD_3)_2SO$) δ 8.09 (q, C-2^1, C-18^1), 10.71 (q, C-7^1, C-13^1), 14.87 (q, C-3^2, C-17^2), 17.19 (t, C-3^1, C-17^1), 19.85 (q, β,β′), 23.83 (t, C-10), 26.91 (d, C-8^1, C-12^1), 40.32 (t, C-8^2, C-12^2), 97.66 (d, C-5, C-15), 121.60 (s, C-8, C-12), 122.55 (s, C-6, C-14), 122.96 (s, C-2, C-18), 123.15 (s, C-7, C-13), 128.03 (s, C-9, C-11), 130.19 (s, C-4, C-16), 147.30 (s, C-3, C-17), 172.08 (s, C-8^3, C-12^2), 173.66 (s, C-1, C-19) ppm. Anal. Calcd for $C_{35}H_{44}N_4O_6$ (616.4): C, 68.16; H, 7.19; N, 9.08. Found: C, 68.13; H, 7.26; N, 8.98.

(−)-(βS,β′S)-Dimethylmesobilirubin XIIIα (1a): From 771 mg (1.2 mmol) of **2a**, as described above for racemic + meso **1**, was obtained 207 mg (28% for both stages) of pure (HPLC) **1a** with $[\alpha]^{20}_D$ −4730° (*c* 0.0086, chloroform). Meso diastereomer **1c** was not found (HPLC) in the crude reaction product.

(+)-(βR,β′R)-Dimethylmesobilirubin XIIIα (1b): From 771 mg (1.2 mmol) of **2b**, as described above for racemic + meso **1**, were obtained 500 mg (68% for both stages) of mixture **1b**–**1c** = 70:30 (HPLC). The diastereomers were successfully separated by column chromatography on silica gel, and after recrystallization from chloroform–methanol ~1:2 v/v was obtained 128 mg of **1c** and 320 mg of **1b** with $[\alpha]^{20}_D$ +4880° (*c* 0.0075, chloroform) both HPLC pure.

Molecular Dynamics. Molecular mechanics calculations and molecular modeling was carried out on an Evans and Sutherland ESV-10 workstation using version 5.41 of SYBYL (Tripos Associates, St. Louis, MO). The dipyrrinone units of **1** were rotated independently about the central $-CH_2-$ at C-10 (torsion angles ϕ_1 and ϕ_2) through 10° increments from 0° to 360°. (The ϕ_1 = 0°, ϕ_2 = 0° conformer has a porphyrin shape.) In this procedure, the two torsion angles were held fixed at each increment while the remainder of the molecule was relaxed to its minimum energy conformation using molecular mechanics. This was followed by a molecular dynamics cooling curve consisting of the following temperatures and times: 100 fs at 20 K, 100 fs at 10 K, 100 fs at 5 K, 200 fs at 2 K, 200 fs at 1 K, 200 fs at 0.5 K, and 300 fs at 0.1 K. This was followed by molecular mechanics minimization, which gave the lowest energy conformations for each set of ϕ values. The conformational energy maps were created using Wingz (Informix), and the ball and stick drawings were created from the atomic coordinates of the molecular dynamics structures using Müller and Falk's "Ball and Stick" program (Cherwell Scientific, Oxford, U.K.) for the Macintosh.

Acknowledgment. We thank the National Institutes of Health (Grant HD 17779) for generous support of this work and Dr. Y. M. Pu for helpful consultations. S.E.B. is on leave from the Institute of Organic Chemistry, Bulgarian Academy of Sciences. R.V.P. gratefully acknowledges awards of an R. C. Fuson Graduate Fellowship and the Wilson Graduate Fellowship. We thank Mr. Lew Cary for invaluable assistance in obtaining NOE data for the ^{1}H-NMR spectra.

Supplementary Material Available: Tables of atomic position and displacement parameters, bond lengths, bond angles, torsion angles, and H-bond geometry (6 pages). Ordering information is given on any current masthead page.